



TAMPEREEN TEKNILLINEN YLIOPISTO  
TAMPERE UNIVERSITY OF TECHNOLOGY

USMAN RASHID  
PARAMETRIZATION OF WINNER MODEL AT 60 GHZ

Master of Science thesis

Examiner: Prof. Markku Renfors  
Examiner and topic approved by the  
Faculty Council of the Faculty of  
Computing and Electrical Eng.  
on January 2015.

# ABSTRACT

TAMPERE UNIVERSITY OF TECHNOLOGY

Master's Degree Programme in Electrical Engineering

**Usman Rashid:** Parametrization of WINNER model at 60 GHz.

Master of Science Thesis, 64 pages

Major: Wireless communication circuits and system.

Examiner: Professor Markku Renfors

Keywords: 60 GHz, channel modeling, parametrization, deterministic field prediction, point cloud, channel measurements, mm-waves.

Future wireless communication systems are calling for increasing data rates and capacity. To achieve the requirements of high capacity and data rates, one possibility is to use large bandwidth. The millimeter-wave frequency band at 60 GHz is one of the good options to address the future data rates and capacity requirements. However, the characterization of wireless channel becomes more challenging as compared to lower frequencies due to the short wavelength in the order of millimeters at 60 GHz. Therefore, in order to characterize the 60 GHz channel, there is a need of more accurate channel models as compared to the existing channel models. The currently recognized and widely used channel models, for instance, 3GPP/3GPP2 Spatial Channel Model (SCM), WINNER, and ITU-R IMT-Advanced are designed for frequencies of up to 6 GHz. They have not been tested on the 60 GHz frequency range. Thus, it is unknown how these channel models will behave at higher frequencies.

In this work, out of several channel models, we have selected WINNER channel model for testing and parametrization at 60 GHz. The reason of selecting the WINNER channel model is that it supports large bandwidth and thus can be a good choice of a channel model that can fulfill the requirements of 60 GHz systems. As a part of WINNER model's testing and parametrization, channel measurements were performed in two different environments, indoor cafeteria and outdoor square. Performing channel measurement is the first step in the creation of channel models. However, real time channel data extracted from the channel measurements is not sufficient to characterize the channel. Therefore, deterministic field prediction based on point cloud method is used to increase the channel data. Based on channel data, some of the important WINNER parameters, such as path-loss and shadowing, delay spread, angular spread, K-factor and delay scaling parameters were extracted, and, as a result, the WINNER model was parameterized at 60 GHz. The parametrization of WINNER model can be used to simulate the behavior of 60 GHz channel in different environments. Furthermore, the parametrization of WINNER model gives us a clear idea about how a particular parameter is changed when the frequency is increased to 60 GHz.

## PREFACE

This Master's thesis has been done in the Department of Radio Science and Engineering, Aalto University, Finland. This work is a small part of METIS project, and it is also reported in one of the METIS deliverables. The METIS project is performed by the METIS partners that include different manufacturers, academic institutions, and research centers. Aalto University is also one of the METIS partners.

First of all, I would like to thank Professor Katsuyuki Haneda for giving me the opportunity to work in the Aalto University and for his help in several issues. I wish to express my gratitude to Markku Renfors, the supervisor of this thesis, who deserves my sincere thanks for his efficient guidance during this thesis. I would like also to thank all the people in the Department of Radio Science and Engineering for keeping up the friendly and educative atmosphere. Especially I want to thank Tommi Rimpiläinen for all his advices and his helpful comments.

Jan Järveläinen have instructed me throughout this work with his great expertise and patience. He deserves my sincere thanks for introducing me to radio wave propagation and channel modeling, helping me with just about everything, encouraging me towards critical thinking and always being available for all issues.

Finally, my family deserves my deepest thanks because without their support and motivation, I would never have finished my studies. Especially, I want to thank my mother who always motivates me to work hard.

Tampere, July 13, 2015.

Usman Rashid.

## CONTENTS

ABSTRACT.....	II
PREFACE.....	III
1. INTRODUCTION .....	1
2. RADIO WAVE PROPAGATION AND CHANNEL MODELING.....	3
2.1. Basic wireless channel and radio wave propagation.....	3
2.2. Channel modeling .....	6
2.2.1 Free space propagation model.....	7
2.2.2 Deterministic models.....	8
2.2.3 Stochastic models.....	9
2.3. Radio propagation and channel modeling at 60 GHz .....	10
2.3.1 IEEE 802.15.3c channel model.....	11
2.3.2 IEEE 802.11ad channel model.....	12
2.4. Future channel models .....	12
3. WIRELESS WORLD INITIATIVE NEW RADIO (WINNER) MODEL .....	13
3.1. Propagation Scenarios .....	13
3.1.1. A1: Indoor .....	14
3.1.2. B1: Urban Microcell .....	16
3.2. Channel modeling approach.....	16
3.3. WINNER Parameters .....	18
3.4. Modeling process .....	19
3.5. Network layout.....	20
3.6. WINNER generic channel model.....	21
3.7. Reduced complexity model.....	22
3.8. Path loss model.....	22
3.9. Channel coefficient generation procedure.....	23
4. CHANNEL MEASUREMENT AND PREDICTION.....	25
4.1. Measurement equipment and sounder configuration .....	25
4.2. Measurement environments at 60 GHz.....	27
4.2.1. 60 GHz channel measurements in outdoor square.....	28
4.2.2. 60 GHz channel measurements in an indoor cafeteria.....	28
4.3. Deterministic field prediction.....	29
5. WINNER PARAMETERIZATION.....	31
5.1. Channel impulse response (CIR).....	31
5.2. Power delay profile and Power angular delay profile.....	31
5.3. Delay spread and distribution.....	33
5.4. Total power .....	34
5.5. Angular spread and distributions .....	34
5.6. Path loss (PL) .....	36
5.7. Shadowing.....	37
5.8. Rician K factor .....	39
5.9. Cross polarization ratio (XPR).....	40

5.10. Cluster parameters .....	41
5.11. Cumulative probability density function plot (CDF plot).....	42
5.12. Auto correlation and cross correlation of large scale parameters. ....	42
6. RESULT AND DISCUSSION .....	43
6.1. Delay spread comparison .....	45
6.2. K-factor.....	47
6.3. Azimuth angular spread (Arrival/Departure) Comparison.....	48
6.4. Elevation angular spread (Arrival/Departure) comparison .....	51
6.5. Number of clusters comparison.....	52
6.6. Path loss and shadow fading .....	53
7. CONCLUSIONS.....	55
REFERENCES.....	56

## ABBREVIATIONS

AOA	Angle of Arrival
AOA	Angle of Departure
AP	Access Point
BS	Base Station
BER	Bit Error Rate
CEPT	European Conference of Postal and Telecommunications Administrations
COST	European Cooperation in Science and Technology
3GPP	3rd Generation Partnership Project
CDL	Cluster delay line
CDF	Cumulative distributive function
DS	Delay spread
5G	Fifth generation
FRS	Multiple relay stations
FCS	Far-cluster scatters
GSCM	Geometry based stochastic channel model
ISI	Inter symbol interference
ITU-R	International Telecommunication Union-Radio communication
IMT-Advance	International Mobile Telecommunication-Advance
LOS	Line of sight
METIS	Mobile and wireless communications enables for twenty-twenty (2020) information society

mm-waves	millimeter-waves
MS	Mobile station
MIMO	Multiple input multiple output
MPCs	Multi path components
NLOS	Non line of sight
OLOS	Obstructed line of sight
PADP	Power angular delay profile
PL	Path loss
PDF	probability density function
RX	Receiver
SCM	Spatial channel model
SCME	Spatial channel model extended
SF	Shadow fading
SNR	Signal to noise ratio
2G	Second generation
FP7	Seventh Framework Program for research and development
TX	Transmitter
TDL	Tapped delay line
3G	Third generation
UTD	Uniform theory of diffraction
VNA	Vector network analyzer
WINNER	Wireless world initiative new radio

# 1. INTRODUCTION

Wireless communications have revolutionized the way we live and do business. In today's world, the users of smart phones and other communication devices, such as laptops and tablets, are increasing at high rates. As a consequence, the demand for higher data rate is also increasing. Furthermore, high network capacity is required to fulfill the demands of future systems. To achieve the elevated network capacity and data rate requirements, one possibility is to use large bandwidth [1]. However, today, the cellular companies are working on frequencies up to 5 GHz in relatively narrow frequency bands, which are not sufficient to meet future needs of bandwidth and data rate requirements. In order to keep pace with these ever-increasing demands, the industry needs to adopt new wireless technologies. These technologies are long-term evolution (LTE), LTE advance, and millimeter-waves (mm-waves) systems. They will help to meet next-generation data rate and bandwidth requirements. Among these technologies, the millimeter-waves frequencies (30-300 GHz), and specifically 60 GHz bands, are attractive for the future ultra-high data rate wireless systems [1, 2]. The 60 GHz range is allocated as a license-free band worldwide. The band from 57 to 66 GHz is in the standardization progress by the European Conference of Postal and Telecommunications Administrations (CEPT); the range from 57 to 64 GHz is available in the United States, Canada, and South Korea; the range from 59 to 66 GHz is available in Japan, and the range from 59 to 63 GHz is available in Australia. Regulations in the United States, Japan, Canada, and Australia have already been set for 60 GHz operation [2, 3].

The performance of the wireless system is highly dependent on the properties of the channel. Therefore, the understanding of channel has the key importance in the deployment of the new systems [2, 3]. For the sake of characterization of the channel, channel models are used. In order to model the channel, knowledge of the multi-path components is required. Consequently, to determine the multi-path components in the environment, the detailed knowledge of the positions and the electromagnetic characteristics of all scatterers in the environment are needed. A lot of research has been done to model wireless communication channel for frequencies up to 10 GHz [4]. However, at 60 GHz channel properties are different from the channel properties at lower frequencies, and the short wavelength makes the channel characterization difficult. The 60 GHz channel has been studied over many decades. However, still new research is required to characterize, evaluate and model the channel at 60 GHz [2, 4].

This work has been done at the Department of Radio Science and Engineering at Aalto University for METIS (Mobile and wireless communications Enablers for Twenty-Two (2020) Information Society) project. METIS is co-funded by the European Commission as an Integrated Project under the Seventh Framework Program for research and development (FP7). The objective of the project is to lay the foundation of the fifth generation (5G) mobile and wireless communication systems so that future data rate and capacity requirements could be met. METIS consists of 29 partners coordinated by Ericsson

[5]. The METIS vision is future where access to information and sharing of data is available anywhere and anytime to anyone. One of the goals of METIS is to propose the channel models for future 5G system development. There are two main factors determining the requirements on the 5G channel models. The first one is the usage scenarios that include various new aspects as compared to the previous 2G, 3G, and 4G, such as ultra-dense networks. The second factor is the difficulty in devising technology that allows signal to propagate at higher frequencies. In this work, we did small contribution to address the propagation challenge.

Currently recognized and widely used channel models, e.g. 3GPP/3GPP2, Spatial Channel Model (SCM), WINNER, and ITU-R, IMT-Advanced are designed for frequencies of up to 6 GHz [5, 6]. At the same time, they are not tested on in 60 GHz frequency range. Therefore, the first task is to select the appropriate channel model that could meet the requirements of 60 GHz system. In this work, out of several channel models, we have selected WINNER channel model for testing and parametrization at 60 GHz. The reason of selecting the WINNER channel model is that it supports large bandwidth [6]. As a part of WINNER model's testing and parametrization, channel measurements were performed in two different environments, indoor cafeteria and outdoor square. Performing channel measurement is the first step in the creation of channel models. However, real-time channel data extracted from the channel measurement is not sufficient to characterize the environment. Therefore, in order to have better structural description of the environment, deterministic field prediction method based on point cloud is used to increase the channel data [7]. Based on channel measurement data, WINNER parameters such as path-loss and shadowing, delay spread, angular spread, K-factor and delay scaling parameters were extracted. The parametrization of the channel model is necessary to create the channel model and to simulate the behavior of 60 GHz channel in different environments.

The rest of this thesis is organized as follows: Chapter 2 provides the background information that is relevant for this work. In this chapter, we first review radio wave propagation, channel, and then we describe the idea of radio channel modeling. Furthermore, this chapter also introduces the radio wave propagation at 60 GHz and reviews some of the existing channel models at 60 GHz. The WINNER channel model is introduced in Chapter 3. The measurement equipment and sounder configuration, which is required to perform 60 GHz channel measurement in different selected environments, is explained in Chapter 4. Chapter 5 explains the WINNER parameters and their extraction procedure, which gives better idea about parameters. The results and analyses of WINNER parameters at 60 GHz are presented in Chapter 6. We conclude the work with a summary of the results and a discussion of the future prospects.

## 2. RADIO WAVE PROPAGATION AND CHANNEL MODELING

### 2.1. Basic wireless channel and radio wave propagation

The basic communication system can be viewed as a link between the source and destination, where the information is sent from the source and received at the destination [8]. The transmitter takes the information from the source and converts it into a suitable form so that it can be transferred over the channel towards the destination as shown in the Figure 2.1.

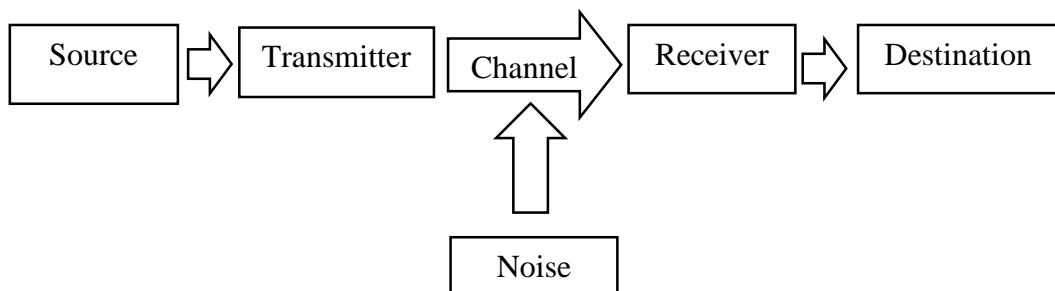


*Figure 2.1: Basic communication system.*

The wireless channel is perceived as a “black box” that is connecting transmitter and a receiver as shown in Figure 2.2. The transmitter launches an input signal X into the channel, and the receiver captures an output signal Y. The signal received by the receiver might not be same as the transmitted signal. The reason of this difference might be because the receiver was moving between the transmissions or the propagation environment changed for some other reasons [9].

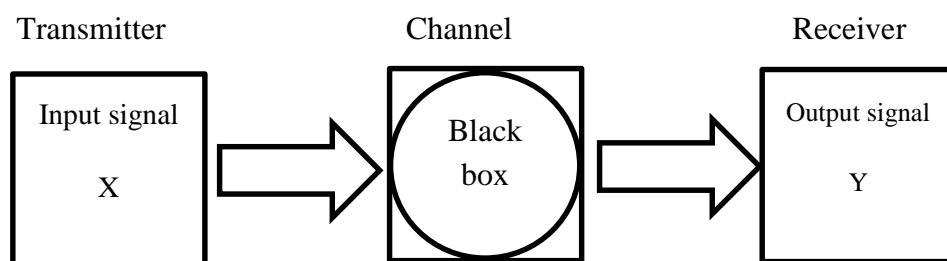


*Figure 2.2: Communication system with transmitter, “black box” wireless channel and receiver.*

The wireless channel can be divided into two types, i.e. radio channel and propagation channel [4]. Figure 2.3 shows the difference between radio channel and propagation channel. In the radio channel the effects of TX and RX antenna, such as antenna gain and polarization mismatch, are included in the channel [4]. On the other hand, propagation

channel describes the effect of the channel without any influences of antennas, and the isotropic antennas are assumed to be used both at the TX and RX, where, isotropic antenna is an ideal antenna which radiated equally in all directions, and it is used as a reference antenna [4].

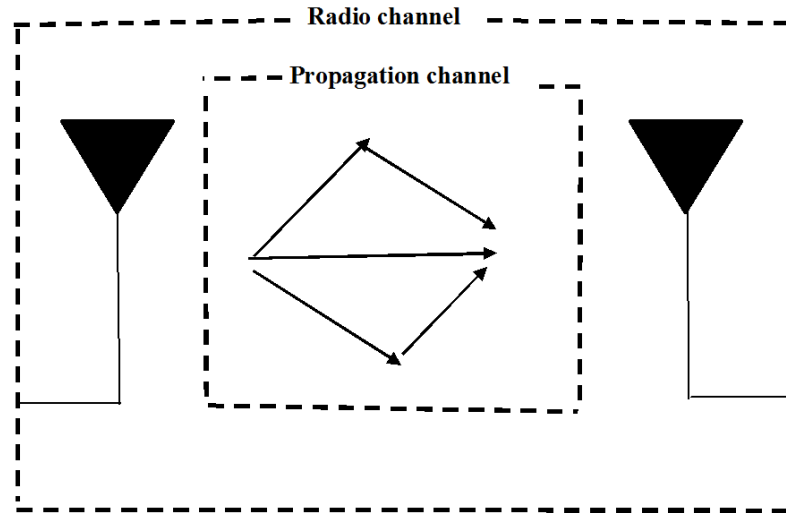


**Figure 2.3: Difference between radio channel and propagation channel.**

In order to develop better concept about the wireless channel and channel modeling, the understanding of radio wave propagation is essential [8]. When a transmitting antenna is excited with a sinusoidal current, it will transmit electromagnetic waves that will interact with the surrounding environment, and will finally excite a current on the receiving antenna. The interaction of the electromagnetic waves with their surrounding is complex, and will strongly depend on the environment [9]. Depending on the particular frequency, the transmitted waves are affected differently i.e. higher the frequency less far they travel and vice versa [9, 10].

Furthermore, the radio waves on their way from transmitter to receiver are affected by the noise. The noise can be divided in to two types: external noise and internal noise. The internal noise is generated within the communication system such as noise generated in the transmitter or receiver. The external noise is generated by external sources which includes the atmospheric effects, cosmic radiations and interference from other nearby appliances and commonly known as additive noise [11]. In radio propagation, the transmitted signal is affected due to multiplicative distortion, and such distortion occurs due to various propagation processes such as reflections, refraction, scattering and transmission. These propagation processes are encountered by the transmitted signals on their way from the transmitter to the receiver [11]. All these phenomena are described below:

*Free space propagation:* In the free space propagation, it is assumed that there are no objects between transmitter and receiver. The attenuation in the free space propagation occurs when the wave propagates away from the transmitter [10, 11].

*Reflection:* The reflection occurs when the electromagnetic wave hits an object that has large dimension compared to the wavelength. In most of the cases, the reflection usually occurs on the smooth and plane surface of buildings and walls. In those cases, the reflection problems are solved by using the Snell's law. The Snell's law of reflection states that the angle of incident wave  $\theta_i$  is equal to the angle of reflection  $\theta_r$ , as shown in Figure 2.3. The incident wave is reflected back to the first medium at an angle  $\theta_r$ , and part of its energy is transmitted at an angle  $\theta_t$  where  $\epsilon$  is the permittivity of the medium and  $\mu$  is the permeability of the medium [10, 11].

*Transmission:* Transmission occurs when the wave propagate through the medium without change in the frequency according to Snell law [10, 11].

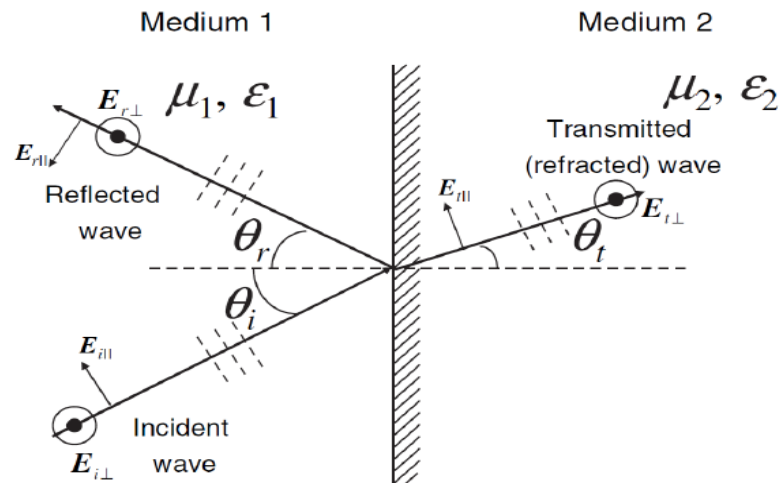


**Figure 2.4: Reflection and transmission [11].**

*Diffraction:* The diffraction occurs when the wave impinges upon the object that has large dimension compared to the wavelength. This phenomenon affects the radio wave propagation, for instance, bending of waves around the corner of an obstacle. Diffraction depends on the geometry of the object and the polarization of the incident wave at the point of diffraction [11, 12].

*Scattering:* Scattering occurs when the wave is forced to deviate from its straight path due to non-uniformities in the medium, and the energy of the radio waves is spread out in many directions. These non-uniformities causing scattering are referred as scatterer. The scattered waves are produced by the rough surfaces, small objects and other irregularities in the propagation path [11, 12].

*Multi-path propagation:* The multi-path propagation is the phenomenon where the radio waves carrying the information bounce on walls, floors and other interacting objects. The transmitted signal reaches the receiving antenna multiple times through distinct paths and at different time instants. The main causes of multi-path propagation include reflections from buildings, mountains, ionosphere reflection, refractions, and so on. The effect of multi-path propagation includes constructive and destructive interference, and phase shifting of the signal [10, 12].

## 2.2. Channel modeling

The channel modeling is basically the characterization of link between transmitter and receiver. The main goal of the channel modeling is to capture the most important aspects of the system. It is used for product design, development, and evaluation of technology proposals. This is more important in the system simulation to reduce the overall simulation time. Furthermore, it is used to simulate certain aspects of what really happens between the transmitter and receiver without need to implement the actual wireless system [1, 9]. One of the important advantages of channel modeling is that they are used to predict the behavior of radio channel in the specific environments without need to perform channel measurements for every scenario, which saves time and effort [14, 15].

The first step in the creation of channel models is performing real time channel measurements to observe the propagation phenomena, then the actual model is designed and parameterized. Furthermore, if needed, more channel measurements are performed in order to increase the channel data to reach a realistic parametrization [16]. Finally, the model is validated according to some pre-defined metric. Thus creating a channel model is a three-step procedure, as shown in Figure 2.5.

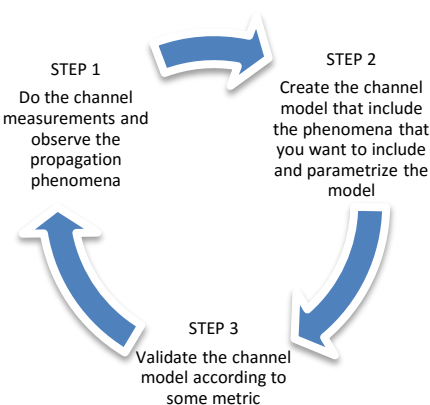


**Figure 2.5: Channel modeling process.**

However, wireless channel modeling is a complicated process due to the propagation phenomena mentioned in the previous section that govern radio wave propagation. This

makes the channel modeling an interesting research subject [14]. Basically, channel models are needed for the testing and analysis of the system performance. The channel models that can accurately describe the propagation channel are required for the planning of the wireless system. Therefore wireless channel modeling implies trade off. On one hand it should be very accurate and on the other hand it should be easy to use. In order to meet the demands of future wireless systems, the new channel models are required to be more versatile and accurate than the existing channel models [4].

There are several types of channel models and selecting the correct channel model depends on the system, environment and its intended use. The existing channel models can be categorized into two main groups: deterministic models and stochastic models [4, 17]. When it comes to choosing an appropriate model, the factors, such as carrier frequency, bandwidth and environment, play an important role [18, 19]. Figure 2.6 shows the classification of the types of channel models.

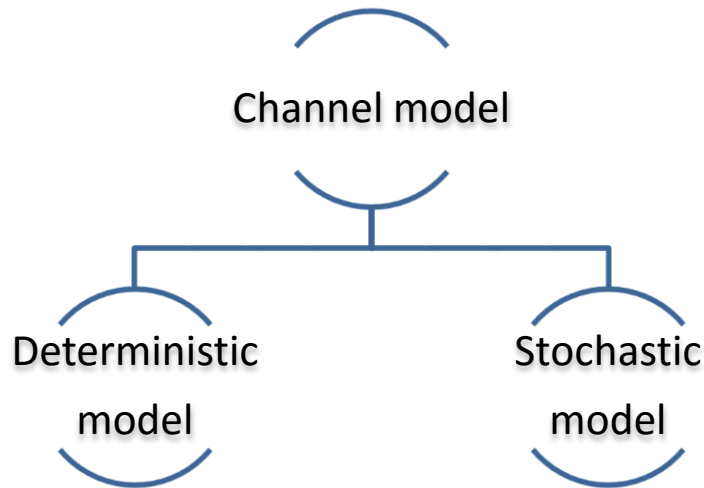


*Figure 2.6: Classification of channel models.*

Further in this chapter we will start with the description of the simplest propagation model, i.e. free space propagation model, and then we will introduce the deterministic models, and stochastic models successively.

### 2.2.1 Free space propagation model

The simplest radio propagation model is the free space propagation model [11]. In this simple radio propagation model, it is assumed that there are no objects between transmitter and receiver. The received power at the receiver, which is separated from the transmitter by a distance  $d$ , is given according to the Friis' law as follows:

$$P_r(d) = P_t G_t G_r \left( \frac{\lambda}{4\pi d} \right)^2, \quad (2.2)$$

where  $P_r(d)$  is the received power at TX-RX separation distance  $d$ ,  $P_t$  is the transmitter power,  $G_t$  and  $G_r$  are the gains of transmitter and receiver antenna respectively,  $\lambda$  is the wavelength. In order to express it as a propagation loss in the free space, (2.2) is rearranged as follows:

$$L = \frac{P_t G_t G_r}{P_r} = \left( \frac{\lambda}{4\pi d} \right)^{-2}. \quad (2.3)$$

The above expression shows the free space path loss and it clearly indicates that the free space path loss depends on the frequency and distance. Expressing the free space path loss in decibels (dB), frequency in GHz and distance in mm, we get the following

$$L = 32.4 + 20 \log R + 20 \log f_{GHz}. \quad (2.4)$$

The above equation indicates that the free space path loss increases with the increase in frequency. [12]

## 2.2.2 Deterministic models

The deterministic description of the radio channel is a difficult task, for instance, suppose one could give a complete description of the propagation environment between a transmitter and a receiver at a certain instant. However, the propagation environment is changed by adding few people or objects and therefore, the radio channel has to be re-determined [9, 14]

Basically, the deterministic channel models are used for complete description of the environment, and therefore, they are site specific. They are based on the electromagnetic wave theory using Maxwell's equations [9]. These models simulate the physical propagation of radio waves, and they directly use the channel measurement data as an input. In order to reproduce the propagation process as accurately as possible, the geometry and electromagnetic characteristics of the given environments are stored. Therefore, the deterministic models are highly accurate, but on the other hand, they require high computation effort. Such models are usually used instead of actual measurement, which needs more effort, money and time. They can also be used when the actual environment is difficult to measure. Moreover, these models are particularly used in the case where high accuracy is required, such as base station placement or coverage analysis for a specific environment [1, 19].

Example of deterministic models is models based on ray tracing techniques. In the ray tracing technique, the received signal is computed from the knowledge of geometry of environment, the electrical property of the medium of propagation, and antenna radiation pattern. The strengths of reflected and transmitted rays are calculated by using geometric optics. The diffracted rays are calculated by the uniform theory of diffraction (UTD). The UTD is the method for solving electromagnetic scattering problems from the small discontinuities or discontinuities in more than one dimension at the same point. The main advantage of this technique is that it is computationally less demanding as compared to deterministic modeling using Maxwell's equation [4, 19]. The models based on the ray tracing techniques are image based models, which assume that all objects in the propagation environment are potential reflectors. It uses an image of the transmitter relative to all reflectors, i.e. all objects in the environment are used to determine the direction of reflected waves. The complexity of the propagation scenario has a strong impact on the computational load since more obstacles in the environment lead to more reflections and diffractions, etc. The advantage of the ray tracing model is that it considers the paths that really exist between transmitter and receiver. On the other hand, the main disadvantage of the ray tracing model is that its computational time grows exponentially with increasing number of reflections [14, 19].

### 2.2.3 Stochastic models

When it is impossible to predict how the radio channel will behave deterministically, it might be possible to determine how the radio channel will behave in a statistical way. For example, it may be impossible to know if my signal level rises or drops at a certain point, but it may be possible to know the magnitude of the variation that can be expected [9].

The stochastic models are used to model the random aspect of channel with random variables, for instance, fading characteristics of the channel, and they model statistically a large number of scenarios with one simulation run. These channel models require little information about the geometry of the environment and they are used for large-scale deployment of the system, which indicates that these models are not site specific [4, 19]. Real time channel measurements are usually performed for stochastic modeling, which captures the impulse response of the channel from the environment. However, performing real time channel measurement is complicated process that requires time and financial resources. The stochastic models have an advantage of describing the wireless channels using simpler approaches that do not require high computational effort compared to deterministic models. In contrast, they might compromise the accuracy, as they do not aim for the complete description of the propagation process [4, 14].

The example of stochastic model is Geometry based stochastic channel models (GSCMs). The GSCMs models are combinations of stochastic and deterministic models. Such models have advantages of both deterministic and stochastic models, e.g. they require less computational time and lower computational load than the deterministic models. However, they are more accurate than stochastic models. The GSCM calculates the received

signal based on the location of scatterers in the propagation environment. The GSCM selects the location of scatters in the stochastic way according to some distribution function [4]. The advantage of GSCM is that they can simulate a large variety of propagation channels for a particular propagation scenario. On the other hand, for specific propagation scenario to find correct propagation parameters associated with that scenario is difficult [9].

Furthermore, one of the important features of GSCM is that different environments can be characterized by changing the input parameters of the model. Therefore, various environments can be simulated with same modeling technique just by changing the parameter sets. However, parametrization of different scenarios is often complicated. Hence, it is difficult to derive the full set of parameters that is required by the channel model [4]. Most of the industry-based channel models follow GSCM models for instance, it is used by WINNER model, 3rd Generation Partnership Project (3GPP), and European Cooperation in Science and Technology (COST) community [4, 11]. These channel models are developed within standardization bodies and proposed by the industry involved in the standardization efforts; they also depend on research efforts by academic institutions.

### **2.3. Radio propagation and channel modeling at 60 GHz**

The radio propagation at 60 GHz is very different as compare to lower frequencies. The main reason for this difference is radio wave attenuation properties. There are several factors that are responsible for the radio wave attenuation, such as high free space path loss (assuming constant gain antennas). Therefore, the transmission over long distance is not possible. The high path loss can be compensated by using directional antennas. However, when such antennas are used, then obstructing Line-Of-Sight (LOS) signal path and misalignments leads to drop in the received power level. This is because the diffraction at the 60 GHz is very weak. On the other hand, the high path loss has the advantage of frequency reuse at short-distances, e.g. inside a room, and therefore, higher data rate can be achieved within the room using same frequency [20].

Furthermore, other factors that are responsible for the radio wave attenuation are because of sharp shadow zones. The sharp shadow zones are created due to small wavelength at 60 GHz compared to the dimensions of physical objects in a room. In order to establish the reliable communication at 60 GHz, these challenges related to propagation characteristics need to be addressed [1, 3].

The design of 60 GHz systems and their standardization require development of reliable channel models. The desired channel model at 60 GHz is required to be a simple model that includes the path loss and radio wave attenuation. However, in the indoor environment, a more general model is required at 60 GHz [4, 20]. In the literature, many 60 GHz models are rooted in the Saleh-Valenzuela (SV) model in which multi-path components arrive in clusters (group of rays) in the delay domain [4]. This model has also been extended to include the angular domain. Most of the recent work on the 60 GHz channel modeling is based on the double-directional modeling approach with modified SV model

that includes delay domain as well as the angular domain [4]. Table 2.1 shows some of the channel models that have been reported at 60 GHz. It clearly illustrates that modeling is moving towards the approach that includes all domains.

**Table 2.1: Different channel models at 60 GHz [4]**

Environments	$\tau$	$\theta_{TX}$	$\theta_{RX}$	$\phi_{TX}$	$\phi_{RX}$	Year
Various	×	—	—	—	—	2005
Laboratory	×	—	—	—	—	2010
Hospital	×	—	—	—	—	2012
Corridor	×	—	—	—	×	2005
Various	×	—	—	—	×	2009
Room	×	—	×	—	×	2009
Various	×	×	×	×	×	2010
Conf.room	×	×	×	×	×	2014

In the above table  $\tau$  is the delay,  $\theta_{TX}$  and  $\phi_{TX}$  are elevation and azimuthal direction of departure (DOD) and,  $\theta_{RX}$  and  $\phi_{RX}$  are elevation and azimuthal direction of arrival (DOA), respectively. Two of the channel models, i.e., IEEE802.11ad and IEEE802.15.3c will be discussed further in this chapter, since they belong in the standard channel models at 60 GHz.

### 2.3.1 IEEE 802.15.3c channel model

IEEE 802.15.3c channel model at 60 GHz was developed and standardized by IEEE802.15.3c working group. It covers several different environments such as office, residential, library, and desktop. For each environment, Line-Of-Sight (LOS) and Non-Line-Of-Sight (NLOS) scenarios are considered. NLOS scenarios are generated from their LOS counterpart by removing LOS components from the model, and the channel parameters are generated. The angular characteristics are considered from the transmitter side [2]. The main drawback of this channel model is that it does not cover most of the wide range scenarios and lacks large measurement data. Besides this, IEEE802.15.3c is a Single-Input-Multiple-Output (SIMO) channel models that includes only azimuth Direction-Of-Departure (DOD) [1, 21].

### 2.3.2 IEEE 802.11ad channel model

IEEE 802.11ad is another installment of 802.11 wireless fidelity (Wi-Fi), and it has a key advantage compared to other 60 GHz standardization activities because it is built on an already strong market presence of Wi-Fi in 2.4/5 GHz bands. The IEEE 802.11ad channel model is more realistic than the 802.15.3c model. This channel model is a MIMO model; it is the mixture of both deterministic and stochastic modeling approaches. The model is parameterized for three indoor scenarios: a conference room, a cubicle, and a living room. Since the model parameters are created deterministically, the parametrization for each scenario is site-specific. Furthermore, this channel model also does not cover large variety of measurement scenarios and lacks large amount of channel data [1, 21].

## 2.4. Future channel models

In order to develop the wireless channel models for the future mm-waves system, we need to find that what is missing in existing channel models. Based on literature survey following needs are identified for the future channel models [5].

- High Bandwidth

The existing channel models are specified for a specific frequency bandwidth that is adequate for currently used frequency range in the industry. However, at higher frequency range, the channel model bandwidth has to be wider.

- Increased number of scenarios

Most of the important propagation scenarios, such as shopping mall, where the density of people may be high, are not covered in the existing channel models. Therefore, there is need to cover more number of scenarios.

- 2D models

Most of the existing models are 2D and they do not cover elevation parameters.

This work is attempt to address the above-mentioned needs and to propose a standard channel model at 60 GHz. Further we will introduce the WINNER channel model in detail.

### 3. WIRELESS WORLD INITIATIVE NEW RADIO (WINNER) MODEL

WINNER channel model is most widely used in modeling the channel at microwave frequencies and the reason of selecting this channel model for 60 GHz system is that it gives reasonable compromise between accuracy and complexity [6, 22]. Furthermore, other characteristics which make the WINNER channel models good candidate for the future 60 GHz system are:

- Support for arbitrary multi-antenna arrays.
- Variable large-scale parameters.
- Wide bandwidth.

In this chapter we will give brief introduction to WINNER channel model. The channel model is a result of a large European collaborative research project. The project was completed in three phases, i.e. I, II and + from 2004 until 2010 [6]. The main goals of the project can be summarized as follows:

- To develop a radio access system that is scalable based on the common radio access technologies with enhanced capabilities as compared to the existing systems.
- In order to minimize cost per bit make efficient use of the radio spectrum.
- The system has to be defined in a new way such that it can be realized through cost competitive infrastructure and terminals.

#### 3.1. Propagation Scenarios

During the WINNER project, comprehensive set of channel models for 12 different propagation scenarios were developed based on the channel measurements that were performed in different environments. The channel measurements are performed to collect the real time channel data. The WINNER “scenario” is based on measurement results that are gathered by several institutions [6, 14]. The propagation scenarios modeled in WINNER are shown in table 3.1.

Based on different environments, the work in project has been divided in between Concept Groups (CG). There were Local Area (LA), Metropolitan Area (MA) and Wide Area (WA) as shown in the Table. The scenarios mentioned in the table cover a wide range of conditions, and most scenarios include separate model for line of sight and non-line of sight conditions. In addition, some scenarios also include sub models. The environments considered here are those found in the urban area of Europe and North America. However, all possible environments and conditions are not covered, e.g. mountains, and hilly rural environments are not covered in the WINNER project [6, 16].

**Table 3.1: Scenarios covered in the WINNER project [16].**

Scenario	Definition	LOS/NLOS	Speed [km/h]	Freq [GHz]	CG
<b>A1</b>	Indoor office/residential	LOS/NLOS	0-5	2-6	LA
<b>In building</b>					
<b>A2</b>	Indoor to outdoor	NLOS	0-5	2-6	LA
<b>B1</b>	Typical urban micro-cell	LOS	0-70	2-6	LA
<b>Hotspot</b>		NLOS			MA
<b>B2</b>	Bad Urban micro-cell	NLOS	0-70	2-6	MA
<b>B3 Hotspot</b>	Large indoor hall	LOS/NLOS	0-5	2-6	LA
<b>B4</b>	Outdoor to indoor micro-cell	NLOS	0-5	2-6	MA
<b>B5a</b>	LOS stat. feeder, rooftop to	LOS	0	2-6	MA
<b>Hotspot</b>	rooftop				
<b>Metropol</b>					
<b>B5b</b>	LOS stat. feeder, street-level	LOS	0	2-6	MA
<b>Hotspot</b>	to street-level				
<b>Metropol</b>					
<b>B5c</b>	LOS stat. feeder,	LOS	0	2-6	MA
<b>Hotspot</b>	below-rooftop to street-level				
<b>Metropol</b>					
<b>B5d</b>	NLOS stat. feeder, above	NLOS	0	2-6	MA
<b>Hotspot</b>	rooftop to street-level				
<b>Metropol</b>					
<b>B5f</b>	Feeder link BS->FRS.	LOS/OLOS	0	2-6	WA
	Approximately RT to RT	/NLOS			
	level				
<b>C1 Metropol</b>	Suburban	LOS/NLOS	0-120	2-6	WA
<b>C2</b>	Typical urban macro-cell	LOS/NLOS	0-120	2-6	MA
<b>Metropol</b>					WA
<b>C3</b>	Bad Urban macro-cell	NLOS	0-70	2-6	-

### 3.1.1.A1: Indoor

The real time channel measurements for *A1: Indoor* scenario are conducted at 2.45 and 5.25 GHz with 100 MHz bandwidth. Figure 3.2 shows the placement of Base Stations (BS) and mobile stations (MS). The BS is assumed to be in the corridor where LOS case occurs. NLOS case occurs between corridor and rooms, and path loss is calculated into

room next to the corridor, where the Access point (AP) /BS is situated. The wall losses are considered to account for the rooms that are farther away from the corridor [16, 23].

The channel measurements for *A1: Indoor* scenario were performed in the Oulu University, Finland. There were two different buildings (Tietotalo and main building) that were measured at 5.25 GHz with 100 MHz bandwidth [17]. In these two buildings, more than 8 BS's were chosen with many distinct routes. It is clear from figure 3.2 that the indoor environment forms a grid where the locations of BS and MS are described by the x y and z coordinates, i.e., x and y coordinates on one floor and x y and z coordinates over multiple floors [23].

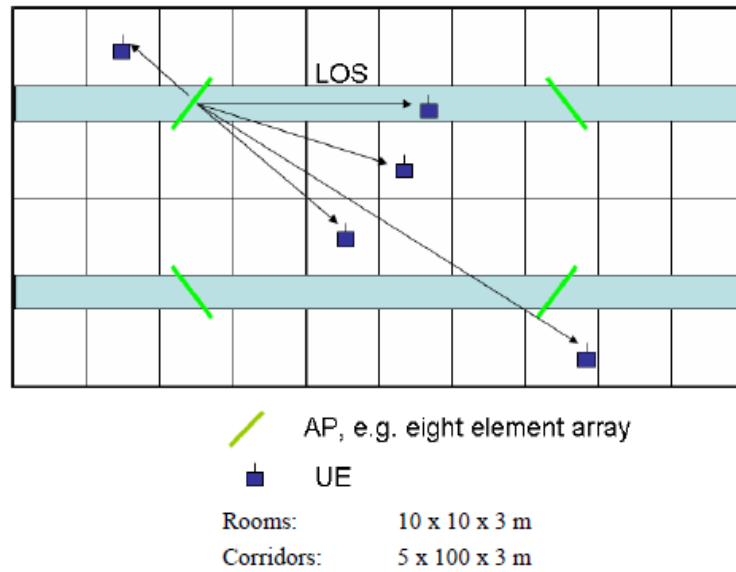


**Figure 3.1: A1: Indoor environment [21].**

Tietotalo is a typical office environment where the corridors are narrow with widths around 1.8 meters. In the university main building, the corridors have different width; the widest is about 3.5 meters. In the room measurements at the university main building, the room size is very close to 10 m by 10 m. Furthermore, in Tietotalo, the sizes of the measured rooms were comparable to 10 m by 10 m. Figure 3.3 shows an indoor environment, where the MIMO measurements were performed in the University of Oulu Tietotalo building [21].



*Figure 3.2: Floorplan and photograph of the measurement site of the 2.45 and 5.25 GHz channel measurements for A1: indoor environment [21].*

### 3.1.2.B1: Urban Microcell

In the urban microcell environment, the height of BS and MS antennas is below the top of the buildings. The BS and MS are in the outdoor environments, where the streets are laid out in a grid. The scenario is defined for both LOS and NLOS case. The “main street” is the street in the coverage area, where there is LOS from all locations to the BS except in the case when LOS path is blocked by the traffic. The streets which intersect the main streets are referred to as the perpendicular streets and those which run parallel to main street are referred as parallel streets. The cell shape is defined by the surrounding buildings. The signal reaches NLOS streets through propagation around the corners, and through and between the buildings [6, 23]. Measurements for urban micro-cellular scenario were taken in the Helsinki city center at 53.GHz center frequency. The used chip rate was either 60 MHz or 100MHz.

## 3.2. Channel modeling approach

The WINNER channel models follow geometric based stochastic modeling approach. This modeling approach has the advantage that it enables the separation of propagation parameters and antennas [16]. The parameters are extracted from the channel measurement data, and they are determined stochastically, based on the statistical distributions. Figure 3.3 illustrates the modeling concept that is used within the (WINNER) framework. The two circles in the figure shows antenna array, the grey rectangular brick shows scatter agent, and black lines shows propagation paths. The channel between each pair of transmit and receive antenna is modelled as a summation of finite number of multipath components (MPCs) referred to as clusters. The term cluster to refer to a group of rays sharing a common delay [14]. The antenna geometries and the field patterns can be defined by the user of the model. These models are based on the clustering concept and therefore, a prerequisite for these models is to have realistic cluster parameters extracted from real

channel sounding data. The cluster is equated with a propagation path diffused in space, either or both in delay and angle domains [6, 16].

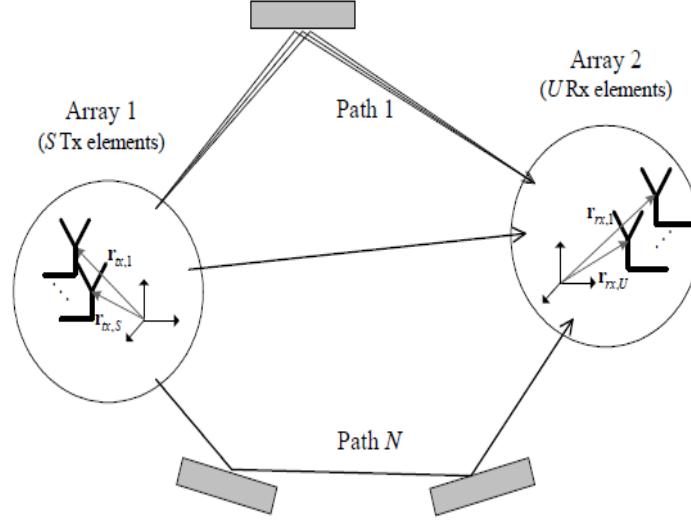


**Figure 3.3: Channel model [16].**

The channels are generated geometrically by summing the contributions of rays and the transfer matrix of the MIMO channel is given by:

$$H(t; \tau) = \sum_{n=1}^N H_n(t; \tau) \quad , \quad (3.1)$$

where  $N$  is the number of clusters. It is composed of antenna array response matrices  $F_{tx}$  for the transmitter,  $F_{rx}$  for the receiver and the propagation channel response matrix  $h_n$  for the cluster  $n$  as follows

$$H_n(t; \tau) = \int \int F_{rx}(\phi) h(t; \tau, \phi, \phi) F_{tx}^T(\phi) d\phi d\phi \quad . \quad (3.2)$$

The channel from TX antenna element  $s$  to Rx element  $u$  for cluster  $n$  is as follows

$$H_n(t; \tau) = \sum_{m=1}^M \begin{bmatrix} F_{rx,u,V}(\phi_{n,m}) \\ F_{rx,u,H}(\phi_{n,m}) \end{bmatrix}^T \begin{bmatrix} \alpha_{n,m,VV} & \alpha_{n,m,VH} \\ \alpha_{n,m,HV} & \alpha_{n,m,HH} \end{bmatrix} \begin{bmatrix} F_{rx,s,V}(\phi_{n,m}) \\ F_{rx,s,H}(\phi_{n,m}) \end{bmatrix} \\ \times \exp(j2\pi\lambda_o^{-1}(\phi_{n,m} \cdot r_{rx,u})) \times \exp(j2\pi\lambda_o^{-1}(\phi_{n,m} \cdot r_{tx,s})) \\ \times \exp(j2\pi V_{n,m}t) \delta(\tau - \tau_{n,m}) \quad , \quad (3.3)$$

where  $m$  is the ray index and  $M$  is the total number of rays inside  $n$ th cluster. Table 3.2 illustrates the corresponding meaning of all the parameters used in the above equation.

**Table 3.2: The channel parameters [16].**

$F_{rx,u,V}$	antenna element $u$ field patterns for vertical polarizations
$F_{rx,u,H}$	antenna element $u$ field patterns for horizontal polarizations
$\alpha_{n,m,VV}$	complex gains for vertical-to-vertical polarizations for ray $n,m$
$\alpha_{n,m,HV}$	complex gains for horizontal-to-vertical polarizations for ray $n,m$
$\lambda$	wave length of carrier frequency
$\varphi_{n,m}$	AoA unit vector
$\Phi_{n,m}$	AoD unit vector
$r_{tx,s}$	Location vectors of element $s$
$r_{rx,u}$	Location vectors of element $u$
$V_{n,m}$	Doppler frequency component of ray $n,m$

### 3.3. WINNER Parameters

The parameters used in a WINNER channel model are divided into Large-Scale (LS) parameters and support parameters. The LS parameters are set first since they are considered as an average over a typical channel segment (distance of some tens of wavelengths). The first three LS parameters are used to control the distributions of delay and angular parameters [6, 16]. Table 3.3 shows list of LS and support parameters.

**Table 3.3: WINNER parameters [6].**

Large Scale Parameters	Support Parameters
Delay Spread and Distribution	Scaling Parameter for Delay Distribution
Angle of Departure Spread and Distribution	Cross-Polarization Power Ratios
Angle of Arrival Spread and Distribution	Number of Clusters
Shadow Fading Standard Deviation	Cluster Angel Spread of Departure
Rican K-factor	Cluster Angel Spread of Arrival
	Per Cluster Shadowing
	Auto-Correlations of the LS Parameters
	Cross-Correlations of the LS Parameters
	Number of Rays per Cluster

All the parameters mentioned in the table above have been specific from the measurement results. It is assumed that the parameters do not depend on the distance. However, this assumption is used for the simplicity of the model [14]. The WINNER parameters will be explained in more detail in Chapter 6. The number of cluster varies from one scenario to another and, the number of rays in the cluster is fixed to 20 in each scenario [16]. Analysis of the measurement data for the different parameters has been described in the Part II document of this deliverable [23].

### 3.4. Modeling process

The WINNER modeling process is divided into three phases as shown in Figure 3.4. The first phase is the definition of scenarios, which indicates the selection of environments to be measured, antenna heights, mobility, and some other general characteristics. Before continuing any further, it is essential to know parameters involved in the channel measurements because these parameters are needed to be measure over each scenario. Subsequently, the measurement data is stored in the database [6, 16].

The second phase begins with the data analysis and post processing. The statistical analysis of this post processed data is carried out to obtain Probability Density Function (PDF) for each parameter. Different analysis methods are applied depending on the parameters that are required. The output from the data analysis block could be path loss data, extracted propagation parameters or a set of impulse responses. The third phase generates the channel model parameters by using PDF. The impulse response matrix is obtained for the parameters and with the antenna information. The generated impulse responses are called channel realizations, which are then used in the simulations. The last part of the modeling process is to simulate each scenario and verify the results by comparing with the data measured in the first phase [16]. The steps that are involved throughout the WINNER modeling process are depicted in Figure 3.4.

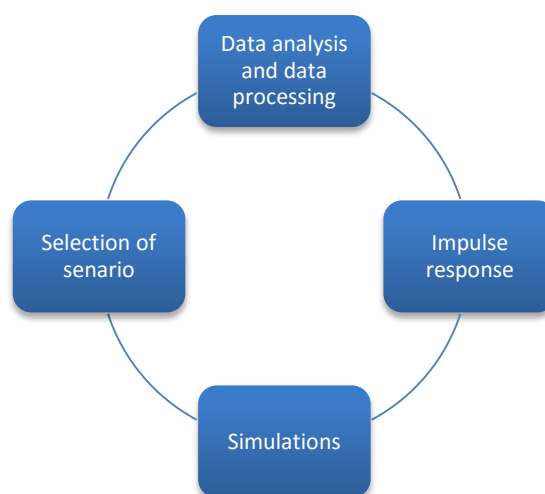


**Figure 3.4:** WINNER modeling process.

### 3.5. Network layout

WINNER channel models enable system-level simulation and testing. This means that many links can be simulated simultaneously. The connection between one MS and one BS's sector is called link [16]. A system-level simulation includes various base stations, several relay stations (FRS), and multiple mobile stations as shown in Figure 3.5. Link level simulation is done for single link, for which the large scale parameters are fixed, shown by the navy blue dashed lines ellipse [6, 16]. The correlation between the large-scale parameters is introduced to obtain correlation between different links. The correlation between the large-scale parameters is a simple function of distance.

Both link and system-level simulations can be done by modeling multiple segments, or by only one Cluster-Delay-Line (CDL) model. The CDL model will be explained further in this chapter. Different segments can be related by correlating the large-scale parameters, but the clusters for one segment are generated specifically for that segment [16].

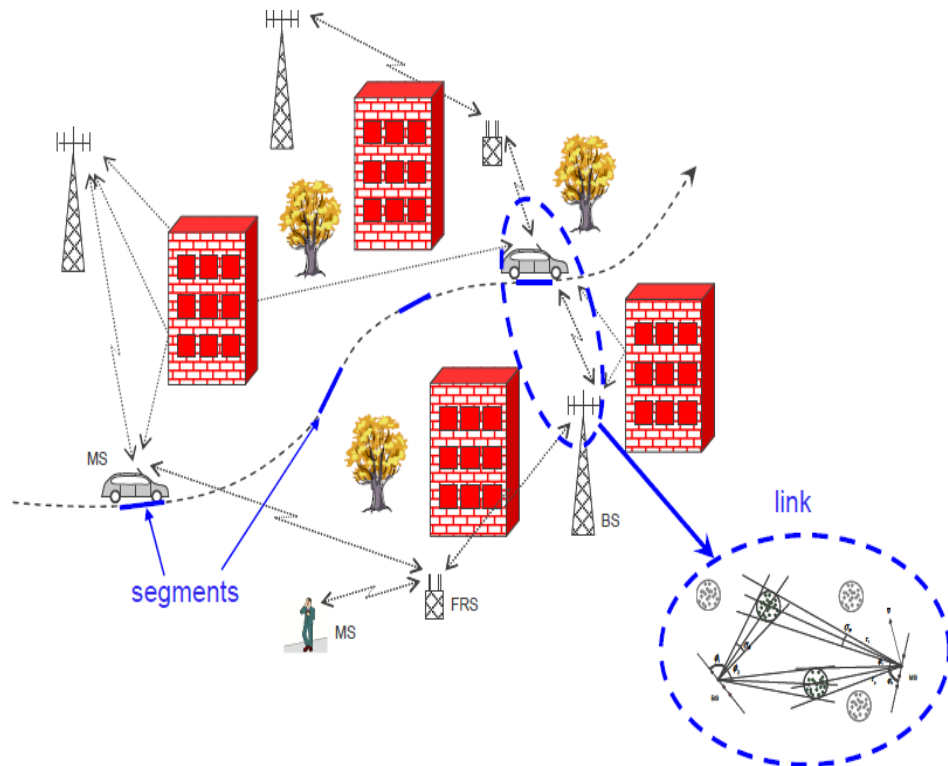


*Figure 3.5: Link level simulation and system level simulation [16].*

Figure 3.6 shows the single link model and also the parameters used in the model. Each circle with several dots represents scattering region. Where  $\Omega$  represents antenna orientation and  $\sigma$  the angular spread. The north (up) is the zero angle reference. In the single link

model, the link is defined by the Multi-Path-Components (MPCs) between two radio stations. At the same time, more complex topologies can be described by the collection of direct radio links [6, 16].

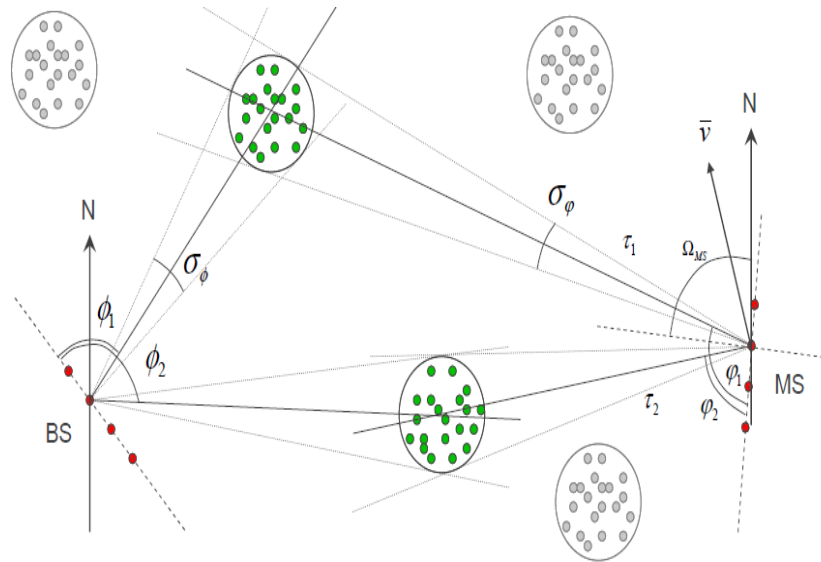


*Figure 3.6: Single link model [16].*

In the multi-link system, some reference coordinate system is required to be established. The reference coordinate system describes the position and movement of the radio station. In general, the positions of the scatterers are unknown and only position of Far-Cluster-Scatters (FCS) is known because they are positioned in the same coordinate system as radio stations. Furthermore, in the multi-link system, the spatial correlation of channel parameters is important. Correlation is caused by the effects of the same scatterers in different links and affect, mainly, the large scale parameter. System level simulation consists of multiple links. In order to develop the correlation between the links at the system level, the parameters are required to be generated in simulations with desired correlation properties [16].

### 3.6. WINNER generic channel model

In the WINNER project, there are two types of channel models: a generic model and reduced complexity model. The reduced complexity model is denoted as the cluster delays line model, which is used for calibration and comparison [6, 16].

The WINNER generic model is a system-level model that can indicate the arbitrary number of propagation environment realizations for either single or multiple radio links for any defined scenarios for desired antenna configurations with one mathematical frame-

work by different parameter sets. There are two or three levels of randomness in the generic model. The first random level is the large-scale parameters like shadow fading, delay and angular spreads, which are chosen randomly from distribution functions. The next level of randomness is the small-scale parameters like delays, powers, directions of arrival and departure, which are determined randomly based on distribution functions and random large-scale parameters (second moments). The large scale parameters are used as control parameters when generating small scale parameters. Geometric setup is therefore fixed in this step and only free variables are the random initial phases of the scatters. An unlimited number of different model realizations can be generated by selecting randomly different initial phases. The model is fully deterministic when the initial phases are fixed [16].

### 3.7. Reduced complexity model

The reduced complexity channel model is used in rapid simulations. The model has an objective of making comparisons between alternative link-level techniques, e.g. modulation and coding choices. These channel models have the characteristics of the famous Tapped-Delay-Line (TDL) models. The TDL models represent the channel by delay line with  $N$  taps. For the determination of fading characteristics, the multi-path angle of arrival and angle of departure information is inherent. For these reasons, the reduced complexity models are also referred to as a cluster delay line (CDL) models [16].

In CDL models, a cluster is centered at each tap. The model is based on a similar principle as the conventional TDL model. However, the difference is that the fading process for each tap is modeled in terms of the sum of rays rather than by a single tap coefficient. The CDL model describes the propagation channel as being composed of a number of different clusters with distinct delays. Each cluster consists of a number of multi-path components (rays) that have same delay value but different angle of arrival and angle of departure. The angular spread within each cluster can be different at MS and BS. The average power, mean AOA, mean AOD of clusters, angle-spread at BS and angle-spread at MS of each cluster in the CDL represent the stochastic model [6, 16].

### 3.8. Path loss model

The path loss models for different propagation scenarios have been developed based on measurement results obtained from several measurement environments [16]. The path loss models are typically of the form.

$$PL = A \log_{10}(d) + B + C \log_{10} \left( \frac{f_c}{5.0} \right) + X \quad , \quad (3.4)$$

where  $d$  is the distance between TX and RX in meters,  $f_c$  is the system frequency in GHz,  $A$  is the fitting parameter, which includes a path loss exponent,  $B$  is the intercept, a fixed quantity based on the empirical observations. It is determined by the free space path loss to the reference distance and an environment dependent constant,  $C$  describes path loss

frequency dependence and  $X$  is an environment specific term [16]. The path loss model can be applied in the frequency range from 2- 6 GHz and for different antenna heights. The free space path loss model that is mentioned in the WINNER document [16] is given by following equation:

$$PL_{Free\ space} = 20 \log_{10}(d) + 46.4 + 20\log_{10}\left(\frac{f_c}{5.0}\right) + X \quad . \quad (3.5)$$

The WINNER path loss model equation clearly shows the dependency on carrier frequency. The path loss models of all environments that are considered in the WINNER model are given in the WINNER document [16]. The WINNER document either defines the variables of (3.4) or provides the full path loss model equation based on measurement results.

### 3.9. Channel coefficient generation procedure

The channel coefficient generation procedure is depicted in Figure 3.7. It gives the minimum description of the system-level channel model.

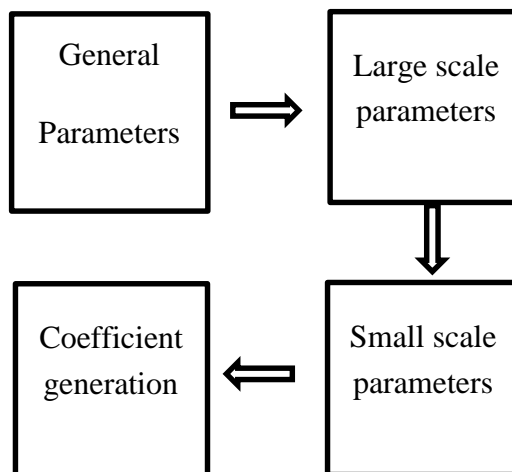


**Figure 3.7: WINNER coefficient generation procedure [16].**

#### *General parameters*

First of all, set the environment, network layout and antenna array parameters then set number of BS and MS, location of BS and MS, antenna field patterns and array geometry, speed and direction of motion of MS and center frequency [16].

#### *Large-scale parameters.*

- Assign the propagation condition such as LOS or NLOS.
- Calculate the path loss.
- Generate the correlated delay spread, angular spread Rician K-factor and shadow fading.

### *Small-scale parameters*

- Generate the delays that are drawn randomly from exponential or uniform delay distribution
- Generate the cluster powers that are calculated assuming a single slope exponential delay profile.
- Generate azimuth arrival angles and azimuth departure angles. However, if power angular delay profile is modeled as wrapped Gaussian, the AOA and AOD are determined by applying inverse Gaussian with input parameters cluster. The same procedure is applied for elevation angles
- Couple randomly the departure ray angles to the arrival ray angles within a cluster
- Generate the polarization power ratio (XPR) for each ray at each cluster. The power angular delay profile and cross polarization ratio will next be explained in more detail in chapter 6.

### *Coefficient generation*

- Draw the random initial phase for each ray at each cluster and for four different polarization combinations. Distribution for the initial phases is uniform
- Furthermore, the channel coefficients are generated for each cluster and each transmitter and receiver element pair according to (3.2). Thus WINNER coefficient generation is four step procedure as shown in Figure 3.7.
- Apply the path loss and shadowing for the channel coefficients

## 4. CHANNEL MEASUREMENT AND PREDICTION

In order to parameterize the WINNER channel model, measurement campaigns are required to be done. The real time channel measurement gives the brief insight of the channel and in our case, it will give insight of 60 GHz channel. In this work, the channel measurements at 60 GHz were performed in two different environments: indoor net café and outdoor square. These channel measurement's campaigns were done in urban areas of Helsinki and Espoo, Finland.

### 4.1. Measurement equipment and sounder configuration

The channel measurement at 60 GHz is different compared to channel measurement at lower frequencies. The main reason for this difference is due to technological constrain of the measurement equipment [4]. The most common equipment to measure the channel response at 60 GHz is vector network analyzers (VNA). VNA is used to measure the scattering S parameters of RF devices, over a wide range of frequencies. It measures the response for the network under test over large bandwidth. The term vector indicates that both the amplitude and the phase of network under test are considered [24].

The real time channel measurements in this work have been done using VNA, up and down converter, a directional horn antenna and omni-directional bi-conical antenna as shown in Figure 4.1. The VNA used for this work sweeps the intermediate frequency (IF) signal from 5 to 9 GHz with 2 MHz frequency spacing. The RF frequencies 61 – 65 GHz are generated with up and down converters and LO operating at 14 GHz. Both TX and RX sides are connected by cables to the VNA. Figure 4.1 shows that the up-converter and transmitter are on a rotator. The measurement's settings are listed in Table 4.1 and the same settings were used in all measurement campaigns performed in this work at 60 GHz.

*Table 4.1: Measurement settings.*

RF frequency	61-65 GHz
LO frequency	14 GHz
IF frequency	5-9 GHz
VNA IF bandwidth	30 kHz
VNA output power	7 dBm
Number of frequency steps	2001
Signal generator output power	18 dBm

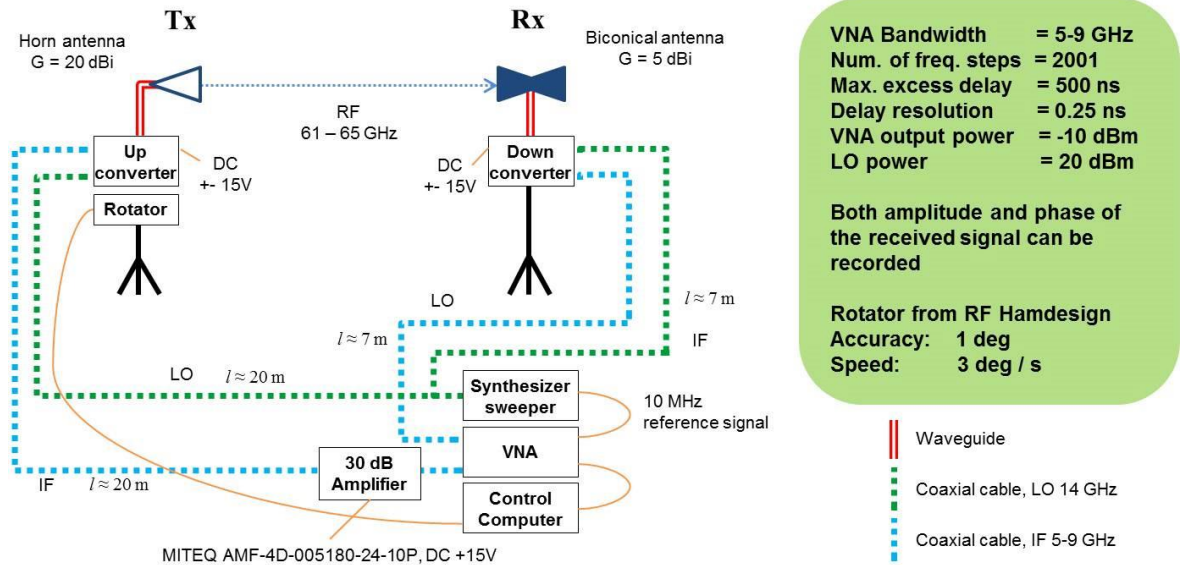


**Figure 4.1: Measurement system and sounder configuration.**

The 20 dBi horn antenna is at the transmitter side, and an omni-directional bi-conical horn antenna with 5 dBi gain is at the receiver side as shown in Figure 4.2. The 4 GHz IF band width leads to a 0.25 ns delay resolution, and the maximum delay is 500 ns. The TX antenna is rotated in the azimuth direction from  $0^\circ$  to  $360^\circ$  with  $3^\circ$  steps.

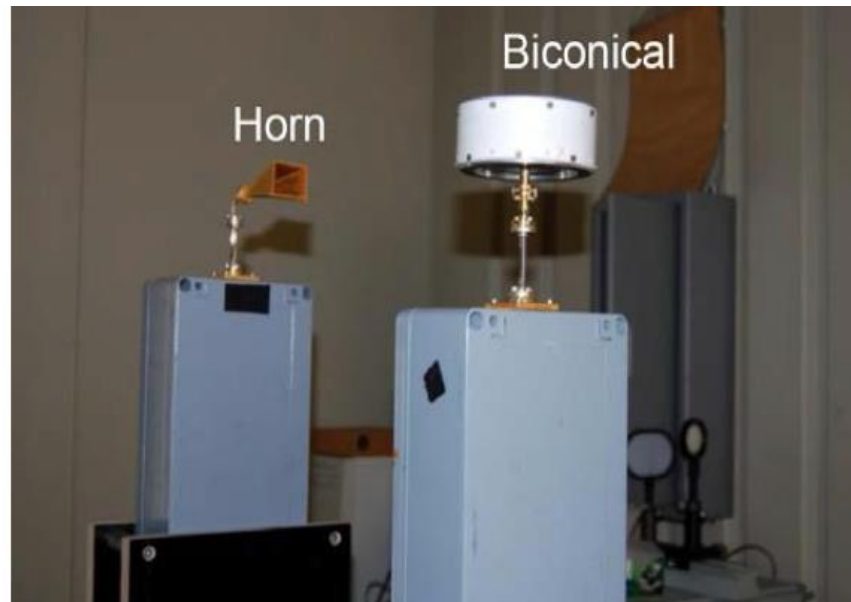


**Figure 4.2: Figure TX (right) and RX (left) antennas.**

A direct back to back calibration is performed to compensate the transfer function of the measurement system. Both amplitude and phase of the received signal are measured at each direction with 2001 frequency steps. Both, TX and RX antennas have relatively narrow elevation plane radiation patterns which limits the measurements to the azimuth

plane. Furthermore, both antennas were vertically polarized and only the co-polarization measurements are done.

## 4.2. Measurement environments at 60 GHz

In this work, the 60 GHz channel measurements were done in two different environments. Table 4.2 shows the propagation environment at 60 GHz. These measurement environments have been specified by the METIS project, and they are found in the urban areas of Helsinki and Espoo in Finland [5].

*Table 4.2: Measurement environments at 60 GHz.*

<b>Propagation scenario</b>	<b>Indoor cafeteria LOS</b>	<b>Outdoor square LOS/OLOS</b>
Link topology	BS-UE	BS-UE
Centre frequency	63 GHz	63 GHz
Bandwidth	4 GHz	4 GHz
Polarization	co- and cross-polarization	co- and cross-polarization
TX location	6 test locations	11 test locations
TX velocity	Stationary	Stationary
TX height above ground level	2 m	2 m
RX location	1 test location	2 test locations
RX velocity	Stationary	Stationary
RX height above ground level	2 m	2 m
TX-RX distance	3 – 7 m	4.5 – 19.2 m
Angular scanning	Rotation in azimuth 0 - 360° with 3° steps	Rotation in azimuth 0 - 360° with 3° steps
Number of measurements	14	15
Remarks	4 LOS and 3 NLOS	12 LOS and 3 OLOS

#### 4.2.1. 60 GHz channel measurements in outdoor square

The channel measurements in outdoor square were performed outside the Kamppi shopping center in Helsinki at 61-65 GHz frequency range. A photograph of the measurement scenario is shown in Figure 4.3.



*Figure 4.3: Measurement site for 60 GHz channel measurements in outdoor square.*

The TX-RX distance is varying between 4.5 and 19.2 m and with TX and RX heights of 2 m. In total, 13 co-polarized and two cross-polarized measurements were performed.

#### 4.2.2. 60 GHz channel measurements in an indoor cafeteria

The channel measurements of the indoor cafeteria were done in the indoor cafeteria of Aalto University, Finland. The cafeteria is located on the ground floor of the building. A photograph of a measurement performed in the cafeteria is shown in Figure 4.4.



*Figure 4.4: Measurement site for 60 GHz channel measurements in cafeteria.*

In total 14 measurements with 1 RX and 6 TX locations are performed. Seven of the measurements are co-polarization and another seven are cross-polarization measurements. Three of the TX locations are in LOS and another three in NLOS.

### 4.3. Deterministic field prediction

The channel data obtain from the real time channel measurement is not adequate to characterize the channel accurately. Therefore, one way to increase channel data is to perform more channel measurements, which are time-consuming and needs financial resources. Therefore, to generate more channel data, the deterministic field prediction methods are needed [7].

Deterministic field prediction methods, such as the point cloud prediction method is one of the methods that further improve deterministic field prediction by providing more accurate structural description of the propagation environment. The point cloud-based propagation prediction method is used to generate more channel data, where accurate descriptions of the propagation environments in the form of a point cloud are obtained through laser scanning [7]. Figure 4.5 shows laser scanning through point cloud prediction method. This method traces the ray from each point.

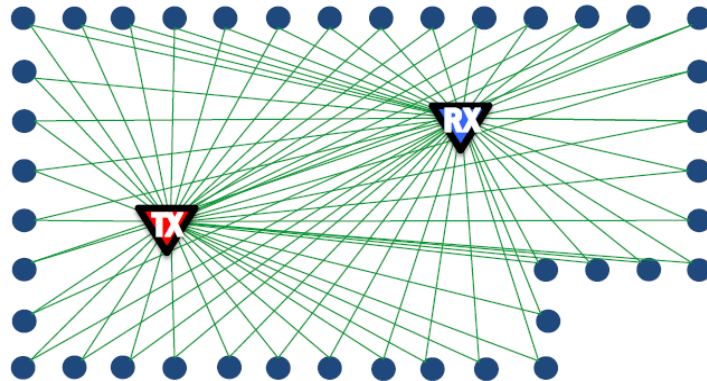


*Figure 4.5: Laser scanning through point cloud prediction.*

The point cloud method uses the single-lobe directive scattering model [25]. The model calculates the backscattering from the point in the point cloud, and the contributions coming from distinct points are combined to give the total field. The reason of using single-lobe directive scattering model is that the spatial sampling rate of laser scanning, which is half the wavelength at 60 GHz [7]. The radio channel environment of interest is estimated as the sum of all signal paths between the transmitter and the receiver. It is assumed that these paths consist of a line of sight (LOS) and single-bounce and double-bounce scattering from each point in the point cloud [25, 26]. The scattering model contains two parameters, a scattering coefficient  $S$  and a scattering lobe width  $\alpha R$ , which relate to the material properties of the local surface.

The characteristics of time-efficient prediction of channels and accurate structural description of environment make this method a suitable candidate for estimating the channel features in the indoor scenarios both in terms of delay and angular characteristics [7, 26]. As an example, the recorded point cloud of the open square (Narikkatori) is illustrated in Figure 4.6.

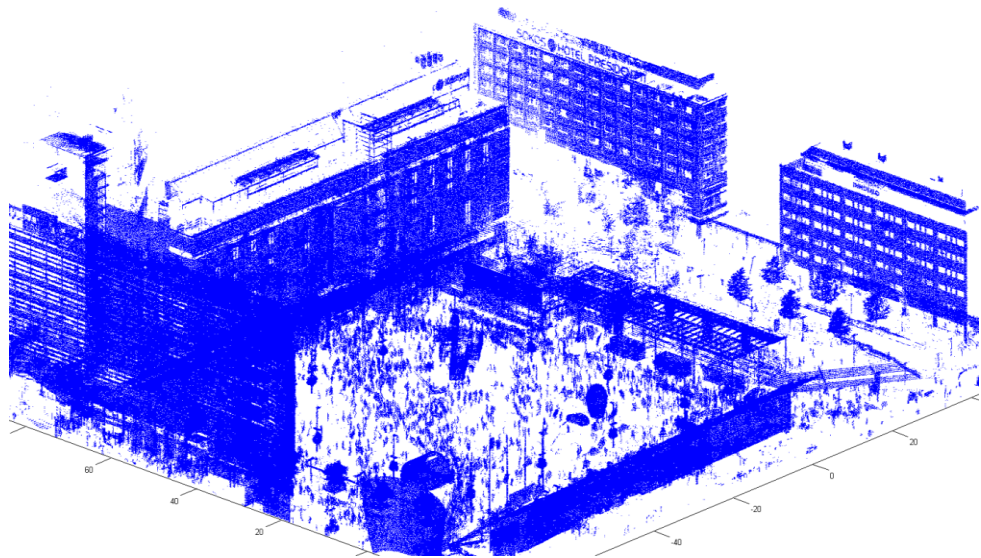


*Figure 4.6: An example of a point cloud.*

## 5. WINNER PARAMETERIZATION

In order to develop the channel model that is based on channel measurement data, the parameters are required to be extracted from the channel data. These parameters are entered in to channel model and in our case, the parameter will be entered in to WINNER channel model. The reproduced channels from the WINNER II model that are generated with our parameters will be compared with measurements, and if they show agreement, then WINNER model is considered to be feasible at 60 GHz for the scenarios in this work. Therefore, the WINNER parameters will be found next in this work. The derived parameters will be based on the channel measurement data and data generated from the point cloud prediction method.

In this chapter, the WINNER parameter extraction method is presented. All the parameters are defined and the meaning of each of them is also explained as rigorously as possible. The parameters includes the large-scale and support parameters that are specified in the WINNER document. They are important in the development of the channel models because they control the behavior of the modeled channel [1]. First, we will start by introducing channel impulse response, Power-Delay-Profile (PDP) and Power-Angular-Delay-Profile (PADP) and then the other parameters will be explained successively. In general, all the parameters can be divided into five groups, related to domain that are calculated from (Delay, Angular), to joint processing of both domains (Cluster), or Polarization, correlation.

### 5.1. Channel impulse response (CIR)

The channel impulse response is a function of time, delay, position of transmitting and receiving antennas and their position given by  $h(t, \tau, s, u, p)$ . Single realization of  $h(\tau)$  is provided for every sub channel  $(s, u, p)$  inside every snapshot. If for instance  $h(\tau)$  does not satisfy the SNR criterion then it would not be used for further processing [23]. Following steps are followed for the extraction of CIR from channel data [23].

1. For each  $(\tau, s, u, p)$  estimate the noise threshold.
2. CIR is valid if the difference between highest peak, and the noise level exceeds the predefined value.
3. Set all values zero that are below the noise level for the valid CIR.
4. There will be valid CIR in the valid snap shot.
5. Form snapshots set as a collection of  $n_t$  consecutive valid snapshots, where  $n_t$  represents that number of snapshots inside stationarity interval.

### 5.2. Power delay profile and Power angular delay profile

The first step in the processing of channel data is to derive the PDP and PADP. The matrix of the channel transfer function is recorded as function of TX rotation angle and as a

function of frequency. Where, PADP is obtained by taking inverse Fourier transform of the channel transfer function matrix. The PDP is derived by the marginal integral of the PADP over the TX pointing directions [22, 24].

Power delay profile is the average power of the channel as the function of excess delay with respect to first arrival path. The number of important parameters such as Delay Spread (DS), Path Loss (PL), Shadow Fading (SF) and the K-factor can be derived from power delay profile. These parameters are useful in the design and implementation of the system [6, 25]. Power angular delay profile defines the average power as a function of angle  $\theta$ , where  $\theta$  is angle of arrival for the receiver and angle of departure for the transmitter. Similar to PDP, the number of angular parameters such as azimuth and elevation spreads can be derived by analyzing PADP [1]. Furthermore, the angles for the detected propagation paths are found from the PADP after the peak detection from the PDP. The path amplitudes are calculated from the path PADP amplitudes taking in to account the effects of antenna gains [24]. Following steps are followed for the extraction of power delay profile from channel data [23].

For each collection of  $n_t$  consecutive valid snapshots, where  $n_t$  represents that number of snapshots inside stationarity interval

1. Calculate the instantaneous power

$$P(t, \tau, s, u, p) = |h(t, \tau, s, u, p)|^2 \quad . \quad (5.1)$$

2. Detect delay corresponding to highest peak.

$$\tau_m(p) = \arg_{\tau} \max( P(\tau, p) ) \quad . \quad (5.2)$$

3. Introduce delay-shift in order to align highest peaks of all CIR components.

$$P(t, \tau', s, u, p) = P(t, \tau - \tau_m, s, u, p) \quad . \quad (5.3)$$

4. Time Variant power delay profile is given by average the instant powers over (TX,RX) dimensions

$$P(t, \tau', p) = \frac{1}{N_s N_u} \sum_{s=1}^{N_s} \sum_{u=1}^{N_u} P(t, \tau', s, u, p) \quad . \quad (5.4)$$

5. PDP is Averaged Time Variant Power delay profile over  $n_t$  snapshots.

$$P(\tau', p) = \frac{1}{n_t} \sum_{i=1}^{n_t} P(t_i, \tau', p), \quad (5.5)$$

where  $n_t$  represents number of snapshots contained inside Stationarity Interval

### 5.3. Delay spread and distribution

Delay spread describes the dispersion of wireless channel in delay domain [1]. It is one of the important parameters of radio propagation that is used to estimate data rate and bandwidth limitations for the multi-path channel. Root mean square (RMS) delay spread is a root square of the second moment of PDP that statistically measures the time dispersion of the channel [27]. It is inversely proportional to coherence bandwidth of the channel. The coherence bandwidth is defined as the range of frequencies over which two frequency components have correlation. It determines whether the system is a narrow or wide band with respect to channel.

A system is narrow-band when the RMS delay spread is less than the symbol period, and coherence bandwidth is larger than the signal bandwidth, and this results in a flat fading channel [2]. In wide-band systems, the RMS delay spread is greater than the symbol period, and coherence bandwidth is less than the signal bandwidth, and hence it results in frequency selective fading channel. A flat fading channel reduces signal-to-noise (SNR) ratio due to deep fading. The frequency selective fading cause's inter-symbol-interference (ISI) that leads to irreducible bit-error-rate (BER) performance [2, 27]. Thus, whether a channel is frequency flat or frequency selective, it does not only depend on the type of environment but also on the type of application [27]. Furthermore, delay spread depends on many other factors, such as the type of environment and antenna directivity. For example, the delay spread is large in the case of large environment where distance between transmitter and receiver is large, and it is small in the case when the distance between transmitter and receiver is small. The antenna directivity affects the delay spread, e.g., the delay spread is small when transmitter and receiver antennas are more directive and vice versa [2]. Following steps are followed for the extraction of RMS delay spread from channel data [23].

In order to extract RMS delay spread from the power delay profile, the following procedure, which is reported in the WINNER deliverable Part II is used in this work [23].

1. Use only the upper 20 dB of the measured PDP. Skip the snapshots that do not provide 20 dB dynamics.

$$P(\tau_i, p) = \begin{cases} P(\tau_i, p) & P(\tau_i, p) \geq \max\{P(\tau_i, p)/100\} \\ 0 & \text{otherwise} \end{cases} . \quad (5.6)$$

2. Estimate the power distribution function from PDP.

$$p(\tau_i, p) = \frac{P(\tau_i, p)}{\sum_{i=1}^N P(\tau_i, p)} \quad . \quad (5.7)$$

3. Calculate first and second moments

$$\tau' = \sum_{i=1}^N \tau_i p(\tau_i, p) \quad . \quad (5.8)$$

$$\tau^2 = \sum_{i=1}^N \tau_i^2 p(\tau_i, p) \quad . \quad (5.9)$$

4. We can calculate the standard deviation (RMS delay spread) by following equation

$$\sigma(p) = \sqrt{\tau^2 - (\tau')^2} \quad . \quad (5.10)$$

#### 5.4. Total power

The total power is sum of power delay profile over  $N_\tau$  delays, where  $N_\tau$  represents the number of samples of CIR in delay domain [23].

$$P(p) = \sum_{i=1}^{N_\tau} P(\tau'_i, p) \quad . \quad (5.11)$$

#### 5.5. Angular spread and distributions

In the multi-path channel, a multi-path component leaves from the transmitter antenna and arrives to the receiver antenna at a specific angle with respect to reference direction. These angles are called Angle-Of-Departure (AOD) and Angle-Of-Arrival (AOA). In order to have full 3D information about the environment, the angles are often defined separately for the azimuth and elevation planes [11, 27].

Angular spread describes the dispersion of radio channel in angular domain .It is the measure of how multi-path signals are arriving or departing with respect to mean angle of arrival or departure [28]. Furthermore, it is related to the space selectivity of the channel, which is measured by coherent distance. The coherent distance for the case of angular spread provides the measure of maximum spatial separation over which the signal amplitude has strong correlation, and it is inversely proportional to the angular spread. The multi-path components that arrive at the receiver with short delays are expected to have smaller angular spread values and vice versa. Smaller angular spread values indicate more

correlations between the TX and RX antennas. In order to achieve full capacity and performance gain of the multi-antenna system, we can use low antenna correlation values [1]. Following steps are followed for the extraction of PADP from channel data [23].

1. For each snap shot reconstruct dependence  $P_i(\phi_i)$  or  $P_i(\varphi_i)$  for the multi-path parameters, where multi-path parameters  $[(\tau_i, \phi_i, \varphi_i)P_i]$  uniquely identifies one multi-path component, where  $P_i$  is power,  $\tau_i$  is delay, and  $(\phi_i, \varphi_i)$  is azimuth information associated with MPC. If elevation information is to be used then multi-path component is described by two additional components  $(\theta_i, \vartheta_i)$ .
2. Average the PADP for all snapshots belonging to the same snapshot set.

Following steps are followed to extract the angular spread from power angular delay profile. This procedure has been reported in the WINNER document [23].

1. Introduce a  $\Delta$  shift to all angles. Mean and standard deviation are shift dependent since wrapping of angles to certain range represents the nonlinear operation.

$$x_i(\Delta) = x_i + \Delta \quad . \quad (5.12)$$

where  $x_i$  can be angle-of-arrival or angle-of-departure.

2. Wrap angles can be azimuthal and elevation where azimuthal is between  $[-\pi, \pi)$  and the elevation angles are in the range  $[-\pi/2, \pi/2)$

$$x'(\Delta) = \text{mod}(x_i(\Delta), WR) \text{ and } WR = \begin{cases} 2\pi & \text{azimutal} \\ \pi & \text{elevation} \end{cases} \quad (5.13)$$

$$\text{if } x'_i(\Delta) > \frac{WR}{2} \rightarrow x'_i(\Delta) = x'_i(\Delta) - WR .$$

3. Estimate the power angular distribution spectrum from power angular spectrum PAS

$$p \text{ as}(x'_i(\Delta), p) = \frac{P(x'_i(\Delta), p)}{\sum_{i=1}^{N_x} P(x'_i(\Delta), p)} \quad . \quad (5.14)$$

4. Calculate the first order moment, i.e., the mean value

$$\text{mean } x'(\Delta, p) = \sum_{i=1}^{N_x} x'_i(\Delta) p \text{ as}(x'_i(\Delta), p). \quad (5.15)$$

5. Subtract mean value from all the angles

$$x''_i(\Delta) = x'_i(\Delta) - \text{mean } x'(\Delta, p). \quad (5.16)$$

6. Perform wrapping of angles

$$x'''(\Delta) = \text{mod}(x''_i(\Delta), WR) \text{ and } WR = \begin{cases} 2\pi & \text{azimutal} \\ \pi & \text{elevation} \end{cases} \quad (5.17)$$

$$\text{if } x'''_i(\Delta) > \frac{WR}{2} \rightarrow x'''_i(\Delta) = x'''_i(\Delta) - WR$$

7. Calculate the second moment.

$$\sigma(\Delta, p) = \sqrt{\sum_{i=1}^{N_x} [x'''_i(\Delta)]^2 p \text{ as}(x'_i(\Delta), p)}. \quad (5.18)$$

8. The angular spread is the minimum value of the standard deviation over  $\Delta$  and we have to repeat all the steps from 1 to 7 in which value of  $\Delta$  is varied until we get minimum value.

$$\sigma_{AS}(p) = \min \sigma(\Delta, p). \quad (5.19)$$

## 5.6. Path loss (PL)

Path loss is the distance and frequency-dependent mean attenuation of the signal [29]. It is the important parameter for the link budget analysis and network planning in order to ensure that the actual system deployment meets the target coverage area. Path loss model predicts the received power level at some distance from the transmitter. In the WINNER model, the path loss models for various environments have been developed as the result of different measurement campaigns [23]. The path loss model equation is given by

$$PL = A \log_{10}(d) + B + C \log_{10}\left(\frac{f_c}{5.0}\right) + X, \quad (5.20)$$

where  $f_c$  is the system frequency in MHz,  $A$  is the fitting parameter including the path loss exponent.  $B$  is the intercept,  $C$  describes the path loss frequency dependence, and  $X$

is an environment specific term. The path loss model with frequency dependency is not yet reported at 60 GHz. Therefore, the distance dependence path loss model is given by

$$PL = A \log_{10}(d) + B, \quad (5.21)$$

For the same type of environments, the value of  $A$  and  $B$  can be different from one case to another. This is due to factors such as the type of antenna, the type of objects present, the layout of the environment, measurement system uncertainties, and the height of the TX and RX antennas, all of which could lead to distinct parameter values [2, 23].

In this work we have used the following steps to extract the path loss from the channel data. It is calculated for each snapshot set from total power [23].

1. For each snapshot, the distance between the transmitter and receiver has to be known

$$P(p) \xrightarrow{d} P(p, d) \quad . \quad (5.22)$$

2. It is also required to find the total transmit power, TX and RX gains and cable attenuation.

$$PL(d, p) = P_{Tx}(p) + \sum_i G_i - \sum_j A_j - P(p, d), \quad (5.23)$$

where  $P(p, d)$  is power at distance  $d$

3. For  $PL(d, p)$  data collected at each measurement level, there is need to perform linear regression. We have used Matlab function *function regress()* for this purpose.

$$\begin{bmatrix} PL(d_1, p) \\ \vdots \\ PL(d_n, p) \end{bmatrix} = \begin{bmatrix} 1 & d_1 \\ \vdots & \vdots \\ 1 & d_n \end{bmatrix} \begin{bmatrix} B(p) \\ A(p) \end{bmatrix} \quad . \quad (5.24)$$

4. The path loss is calculated by following equation:

$$PL(d, p)_{model} = A(p) \log_{10}(d) + B(p) \quad , \quad (5.25)$$

where the values of  $A(p)$  and  $B(p)$  comes directly from linear regression.

## 5.7. Shadowing

Shadowing indicates the variations of average received signal power about its mean, which is generated by the path loss. It is caused by the objects between the transmitter and receiver that attenuate signal power through transmission, reflection, scattering, and

*diffraction* [11, 32]. Basically it signifies the average power received over the large area. Due to variation in the environment, the received power is different from the mean value and in this way shadowing gives the information about the path loss variation about its mean. It is determined by the local mean of the received signal, i.e. the received power is averaged over some particular range. Shadowing is commonly assumed to follow the log-normal distribution given by

$$G(x) = \frac{1}{\sqrt{2\pi}} e^{-\frac{(x-\mu)^2}{2\sigma^2}}, \quad (5.26)$$

where  $x$  is in dB and it is a random variable,  $\mu$  is mean and it is distance dependent path loss and  $\sigma$  is standard deviation of  $x$  which varies with frequency and environment. The value of standard deviation depends on type of environment especially number of objects in the environments, human activities, etc. Figure 5.1 shows the difference between path loss, shadowing and multi-path [32].

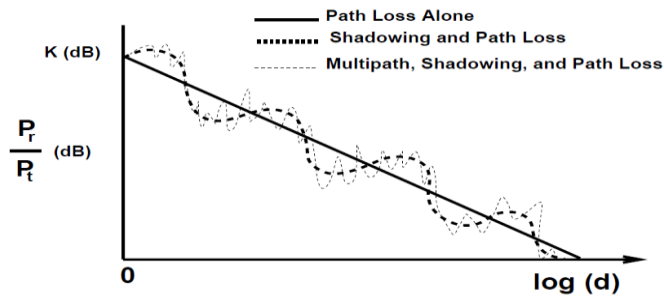


**Figure 5.1: Path-loss, shadowing and multi-path [32].**

Following steps are followed for the extraction of shadowing [23].

1. For the data points  $PL(d_n, p)$   $n = 1, \dots, N_{SE}$  calculate the deviation from the expected path loss  $PL'(d_n, p)$ . Both  $PL$  and  $PL'$  are dimensionless.

$$SF_n(p) = PL(d_n, p) - PL'(d_n, p). \quad (5.27)$$

2. Estimate the mean value of standard deviation for complete measurement set over all snapshots.

$$\sigma_{SF}(p) = \sqrt{\frac{1}{N_{SE} - 1} \sum_{n=1}^{N_{SE}} [SF_n(p)]^2}. \quad (5.28)$$

## 5.8. Rician K factor

The amplitude distribution of small scale fading is characterized by the Rician distribution when there is a strong LOS component present and by Rayleigh's distribution when there is no line of sight signal [11, 23]. The Rician K factor is the ratio of LOS signal power to the total power of all multi-path components. The Rician K factor is given by

$$K = \frac{A^2}{2\sigma^2} , \quad (5.29)$$

where  $\sigma$  is the total power of all multi-path components and  $A$  is peak amplitude. The case  $K = 0$  (no fixed component) corresponds to the most severe fading, and in this limiting case, the gain magnitude is said to be Rayleigh distributed. In the WINNER model, the Rician K factor is estimated using the moment method from which the Rician distribution is deduced [30]. Larger values of Rician K factor indicate stronger LOS component in the channel. The K-factor is either related to narrow-band or wide-band observations; narrow band K factor is used in the WINNER model. The Rician probability distribution is often used to model the fading of the signal strength in a wireless channel in an indoor context. It is used to evaluate the probability that the signal strength is above the minimum requirement which is needed for good communication [11].

In order to extract the narrow band K-factor moment method is used in this work. The narrow band K- factor by moment method is valid only for the calculation of narrowband K-factor i.e. calculated values are appropriate for frequency segments narrower than the coherent bandwidth of the channel, when averaging period is longer than coherent time of the short-term fluctuations. If this property is to be analyzed for selective fading channels then separate analysis is required to be performed per frequency bins narrower than coherent bandwidth [23].

1. Calculate the instantaneous power of CIR.

$$P_i = |h_i(t)|^2, \quad (5.30)$$

where Narrowband (partial) CIR from i-th bin is  $h_i(t)$

2. From the instantaneous power, calculate mean and variance.

$$E\{P_i\} = \frac{1}{n_t} \sum_{i=1}^{n_t} P_i , \quad (5.31)$$

$$\text{Var}\{P_i\} = \frac{1}{n_t - 1} \sum_{i=1}^{n_t} (P_i - E\{P_i\})^2, \quad (5.32)$$

3. Calculate the standard deviation

$$\sigma_i = \sqrt{(E\{P_i\})^2 - Var\{P_i\}} . \quad (5.33)$$

4. K factor is calculated by

$$K_i = \frac{\sigma}{m - \sigma} . \quad (5.34)$$

5. If distance information is available for all measurement set then we can approximate dependence of K-factor over distance by linear regression.

$$K_i(dB) = C_i + D_i \cdot d[m] . \quad (5.35)$$

### 5.9. Cross polarization ratio (XPR)

The cross-polarization ratio  $XPR_V$  vertical is defined as the ratio of power received from vertical to vertical polarization to the power received from vertical to horizontal polarization as

$$XPR_V = \frac{P_{VV}}{P_{VH}} . \quad (5.36)$$

$XPR_H$  horizontal is defined as the power ratio between horizontal to horizontal and horizontal to vertical components.

$$XPR_H = \frac{P_{HH}}{P_{VH}} . \quad (5.37)$$

The XPR values are extracted from the estimated propagation paths using the strongest path (LOS) and the reflected paths (scattering) [23].

Following steps are followed to extract XPR:

1. The ROW of the XPR matrix, i.e., the first index of the XPR elements corresponds to the TX polarization. While the column matrix i.e. the second index corresponds to the RX polarization.

$$XPR = \begin{bmatrix} 1 & \frac{P_{VV}}{P_{VH}} \\ \frac{P_{VV}}{P_{VH}} & 1 \end{bmatrix} , \quad (5.38)$$

where  $P_{VV}$  is power vertical-vertical and  $P_{VH}$  is power vertical-horizontal.

2. If the normalization of power is required at the RX side, the following expression is used. It should be noted that sum of row elements is equal to 1.

$$(XPR)^{-1} = \begin{bmatrix} \frac{P_{VV}}{P_{VV} + P_{VH}} & \frac{P_{VH}}{P_{VV} + P_{VH}} \\ \frac{P_{HV}}{P_{VV} + P_{VH}} & \frac{P_{hh}}{P_{VV} + P_{VH}} \end{bmatrix}. \quad (5.39)$$

### 5.10. Cluster parameters

In channel modeling, cluster is the group of multi-path components that have similar delays and angular parameters [14]. The method to identify clusters is called clustering, and in the WINNER channel model uses the cluster concepts in which all parameters associated with them are considered small-scale parameters like: number of cluster, cluster angle of departure spread, cluster angle of arrival spread, cluster shadowing and number of rays per cluster. This last parameter is fixed to 20 for all WINNER scenarios. However, the number of clusters varies for different environments [6].

The two widely used methods for clustering are: parameter based clustering and clustering based on deterministic field prediction method such as ray tracing [24]. The cluster parameters are used in the channel model to generate new clusters. The cluster parameters may depend strongly on one another. This correlation must be taken into account in channel modeling. The Cluster parameters is one of the important sets of parameters from channel modeling point of view. In order to model the channel in a realistic way, it is necessary to investigate the number of clusters [31]. The number of clusters depends on many factors such as the environment and the number of objects in the environment. Larger number of objects indicates a large number of clusters [14, 23].

Following steps are followed for the extraction of number of clusters:

1. For each snap shot every cluster is represented by centroid [23]. When centroids are calculated, power weighting is used

$$(\tau', \varphi', \vartheta')_n \quad n = 1 \dots N \quad (5.40)$$

2. Apply clustering algorithm to multi-path parameters, which will sort those into N group clusters. Adaptive algorithm that does not use predefined number of clusters that should be used. New clusters should be introduced when distance measure to the existing clusters exceeds predefined value and maximum allowed number of cluster is not reached. Time Variant PDP can also be used to detect resolvable peaks in delay domain.

$$(\tau', \varphi', \vartheta')_i \in C_n \quad (5.41)$$

where  $C_n$  is the clustering algorithm.

3. When clustering procedure has finished number of clusters N for current snap-shot is also known. Estimate the joint Distributions, PADP, angle spread per

cluster which is the same as for whole set of multi-path component and the only difference is that the subset of MPC is considered. All these items are estimated once per stationarity interval.

### 5.11. Cumulative probability density function plot (CDF plot)

In order to examine the distribution of data samples, the CDF plots are commonly used [23]. The approximation of CDF is done from input data samples

1. Approximate the CDF plot by using the ordering position. The ordering of CDF is done through x-sorted.

$$cdf(x\_sorted(i)) = \frac{i}{\#x\_sorted} . \quad (5.42)$$

2. Plot the CDF using the Matlab function stairs (). When more data points are available, the CDF plot will be smoother.

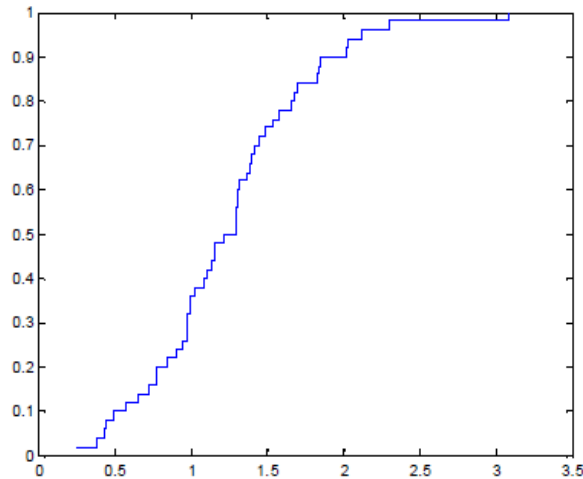


*Figure 5.2: CDF plot [23].*

### 5.12. Auto correlation and cross correlation of large scale parameters.

Auto correlation measures the similarity between a signal and its shifted copy and the cross-correlation measures the similarities between two independent parameters [23]. If two parameters are similar, then the correlation coefficient is 1, if they are different, then the coefficient is 0, and if they are same except that the phase shifted by 180, subsequently the correlation coefficient is -1. The cross correlation in the WINNER model is given by

$$\rho_{xy} = \frac{C_{xy}}{\sqrt{C_{xx}C_{yy}}} , \quad (5.43)$$

where  $C_{xy}$  is the cross-covariance of the LS parameters x and y.

## 6. RESULT AND DISCUSSION

In this work the WINNER parameters are extracted based on the channel data. The extracted parameters are important in the development of the channel model because these parameters are input to the channel model. The generated channels from the channel model are compared with the parameters generated from the measurements. Hence, in this way we can validate the WINNER channel model.

The WINNER channel model in this work is parameterized for two environments: indoor cafeteria, and outdoor square. The parametrization for the indoor cafeteria and outdoor square are based on point cloud field prediction. The point cloud field prediction simulations are calibrated with measured channels. Additionally, the elevation parameters for the WINNER model are provided for indoor cafeteria and for the outdoor square in order to give full 3D information about environment. The WINNER parameter table is derived for indoor cafeteria LOS, obstructed-LOS (OLOS) due to pillars and NLOS case. Similarly, for the outdoor square the parameter table is derived for LOS and NLOS case as shown in Table 6.1. Delay spread and azimuth angular spreads are calculated from the cluster amplitudes, delay, and angles that are generated by the WINNER II implementation. Furthermore, 20 dB dynamic range limit has been used for all the measurements and simulations. The parametrization is based on channel measurements with a 4 GHz bandwidth which gives good delay resolution and allows us to detect the propagation paths directly from the measurements.

In addition, table also contains results of *A1: indoor* scenario shown in light blue color, in order to compare the parameters at 60 GHz with 2.45 and 5 GHz. The WINNER parameter for *A1: Indoor* environments is derived based on the measurement performed at 2 and 5 GHz. In the table  $\sigma$  and  $\mu$  represents standard deviation and mean.

**Table 6.1: WINNER parametrization at 60 GHz and 2.45 GHz.**

Environments		Indoor Cafeteria			Outdoor square		A1: Indoor	
		LOS	NLOS	OLOS	LOS	OLOS	LOS	NLOS
Path loss (PL) PL = A log <sub>10</sub> (d[m]) + B	A	15.94	3.02	7.89	20.3	26.2	18.7	20
	B	66.85	84.41	83.94	67.5	70.5	46.8	46.4
Delay spread (DS) log <sub>10</sub> ([s]) / [ns]	$\mu$	-8.28 /5.57	-8.13 /11.80	-7.93 /8.40	-8.82 /2	-7.72 /23	-7.42 /3.8	-7.60 /2.5
	$\sigma$	0.16 /1.8	0.17 /2.14	0.083 /3.12	0.37 /3	0.32 /11	0.27 /1.86	0.19 /1.54
AoD spread (ASD) log <sub>10</sub> ([°]) / [°]	$\mu$	-7.41 /46	1.51 /73	-7.14 /47	1.10 /27	1.49 /39	1.64 /43	1.73 /53
	$\sigma$	0.29 /24.87	0.26 /10.68	0.06 /22.97	0.75 /21	0.35 /23	0.31 /2	0.23 /1.69

<b>AoA spread (ASA)</b> <b>log10([°]) / [°]</b>	$\mu$	-7.47 /36.25	1.82 /67.95	-7.17 /61.78	0.24 /4	1.31 /30	1.65 /44	1.69 /49
	$\sigma$	0.19 /14.67	0.12 /12.87	0.085 /19.21	0.54 /7	0.44 /22	0.26 /1.81	0.14 /1.3
<b>EoD spread (ESD)</b> <b>log10([°]) / [°]</b>	$\mu$	-7.69/ 21.69	1.03/ 17.41	-7.77/ 14.79	0.43/ 3	0.74/ 7	0.88/ 7.7	1.06/ 11.4
	$\sigma$	0.15/ 8.23	0.17/ 4.19	0.10/ 7.73	0.29/ 2	0.32/ 6	0.31/ 2	0.21/ 1.62
<b>EoA spread (ESA)</b> <b>log10([°]) / [°]</b>	$\mu$	-7.75/ 20.13	1.207/ 18.23	-7.77/ 18.18	0.77/ 12	0.95/ 12	0.94/ 8.7	1.10/ 12.5
	$\sigma$	0.22/ 9.6	0.24/ 6.68	0.17/ 6.71	0.96/ 10	1.19/ 6	0.26/ 1.81	0.17/ 1.47
<b>Shadow fading (SF) [dB]</b>	$\sigma$	1.15	1.07	2.82	0.3	3.5	3	4
<b>K-factor (K) [dB]</b>	$\mu$	-2.09	-12.86	N/A	8.4	N/A	7	N/A
	$\sigma$	2.72	3.68	N/A	2.2	N/A	6	N/A
<b>Cross-Correlations</b>	<b>ASD[°]</b> <b>vs</b> <b>DS[s]</b>	0.01	-0.12	0.31	-0.1	0.4	0.7	-0.1
	<b>ASA[°]</b> <b>vs</b> <b>DS[s]</b>	0.43	0.63	0.07	0.3	0.3	0.8	0.3
	<b>ASA[°]</b> <b>vs</b> <b>SF[dB]</b>	0.15	0.39	0.04	-0.2	0.1	-0.5	0.4
	<b>ASD[°]</b> <b>vs</b> <b>SF[dB]</b>	-0.34	-0.14	0.14	-0.6	0	-0.5	0
	<b>DS[s]</b> <b>vs</b> <b>SF[dB]</b>	0.56	0.24	0.25	0.1	0.5	-0.6	-0.5
	<b>ASD[°]</b> <b>vs</b> <b>ASA[°]</b>	-0.23	-0.11	-0.54	-0.3	-0.2	0.6	-0.3
	<b>ASD[°]</b> <b>vs</b> <b>K[dB]</b>	-0.57	0.02	N/A	-0.5	N/A	-0.6	N/A
	<b>ASA[°]</b> <b>vs</b> <b>K[dB]</b>	-0.05	-0.20	N/A	-0.2	N/A	-0.6	N/A
	<b>DS[s]</b> <b>vs</b> <b>K[dB]</b>	0.03	-0.20	N/A	-0.1	N/A	-0.6	N/A
	<b>SF[dB]</b> <b>vs</b> <b>K[dB]</b>	0.77	-0.29	N/A	0.9	N/A	0.4	N/A
	<b>ESD[°]</b> <b>vs</b> <b>DS[s]</b>	-0.59	0.27	0.04	0	0.1	0.5	-0.6
	<b>ESA[°]</b> <b>vs</b> <b>DS[s]</b>	-0.42	0.47	0.20	-0.2	-0.2	0.7	-0.1
	<b>ESA[°]</b> <b>vs</b> <b>SF[dB]</b>	-0.15	-0.14	-0.15	0	0.3	-0.1	0.3
	<b>ESD[°]</b> <b>vs</b> <b>SF[dB]</b>	-0.41	-0.09	0.10	-0.5	-0.1	-0.4	0.1

	<b>ESD[°]</b> vs <b>ESA[°]</b>	0.51	0.11	0.08	0.1	0.2	0.4	0.5
	<b>ESD[°]</b> vs <b>ASD[°]</b>	-0.15	-0.02	0.59	0.4	0.6	N/A	N/A
	<b>ESD[°]</b> vs <b>ASA[°]</b>	-0.32	-0.18	-0.52	0	-0.2	N/A	N/A
	<b>ESA[°]</b> vs <b>ASD[°]</b>	-0.53	-0.29	-0.05	-0.4	-0.1	N/A	N/A
	<b>ESA[°]</b> vs <b>ASA[°]</b>	0.01	0.42	0.13	0.2	-0.2	N/A	N/A
	<b>ESD[°]</b> vs <b>K[dB]</b>	0.03	-0.06	N/A	-0.5	N/A	N/A	N/A
	<b>ESA[°]</b> vs <b>K[dB]</b>	0.30	-0.11	N/A	0.2	N/A	N/A	N/A
<b>Number of clusters</b>		16	34	39	4	25	12	16

Further in this chapter, we will analyse some of the important WINNER parameter at 60 GHz for indoor cafeteria. This analysis gives us a clear idea about how much the particular parameter is changed when the carrier frequency is increased to 60 GHz in the indoor environment.

## 6.1. Delay spread comparison

The delay spread is one of the important parameter to describe the multipath characteristics of the radio channel. Root Mean Square (RMS) delay spread can be calculated from analyzing PDP. The PDPs were derived from the measured transfer functions using the inverse Discrete Fourier Transform with a Gaussian window function to reduce the side lobe level. The cumulative distribution functions of delay spread for indoor cafeteria with LOS, NLOS and OLOS are shown in Figure 6.1

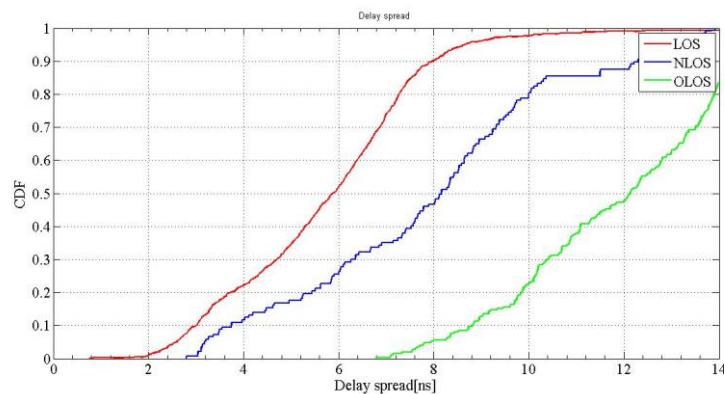


**Figure 6.1.** A CDF comparison of RMS DS LOS, NLOS.

Several observations can be made by analyzing table 6.1 for delay spread values and Figure 6.1. First observation that can be made is that delay spread is small in LOS case as compare to NLOS and OLOS. The main reason for this trend is because in OLOS case, the LOS path is obstructed by the wall, which is the dominant multi-path component and thus this results in the large delay spread values. The values of delay spread are not identical for various types of walls, it is because material properties affect the propagation. Therefore, delay spread might not be the same for different walls made from different materials. Furthermore, by comparing indoor cafeteria delay spread values with that of outdoor square we can observe that delay spread values for the outdoor square OLOS case are quite high. This proves the fact that delay spread depends on the type of environment and typically its values are small for the indoor environments as compared to outdoor environments, which are more densely populated.

In addition if we compare the delay spread values of *A1: Indoor* environment with the cafeteria and outdoor square at 60 GHz, we can easily figure out that in *A1: Indoor environment*, the delay spread values are high. There can be several reason for the small delay spread. First reason could be that in our case, there were no large number of objects and human interference. Second reason could be due to type of antenna used. As we know that delay spread depends on the directivity of the antenna and it increases, when antennas both at TX and RX are not directive. Therefore, we can make analysis that at particular distance the TX and RX antennas are more directive, which leads to reduction in the delay spread values. However, such reduction in delay spread is only noticeable when the TX and RX antenna patterns are aligned to the most significant angle of departure and angle of arrival, respectively. As the misalignment increases, the delay spread will start to increase even if directive antennas are used at TX and RX.

Figure 6.2 shows delay spread as a function of link distance. Figure clearly shows that delay spread increases as the link distance increases. However, in all the three cases we can observe that at particular distance delay spread value decreases. This might be because at that particular link distance the TX and RX antenna patterns are aligned to the most significant AOD and AOA which leads to reduction in DS value.

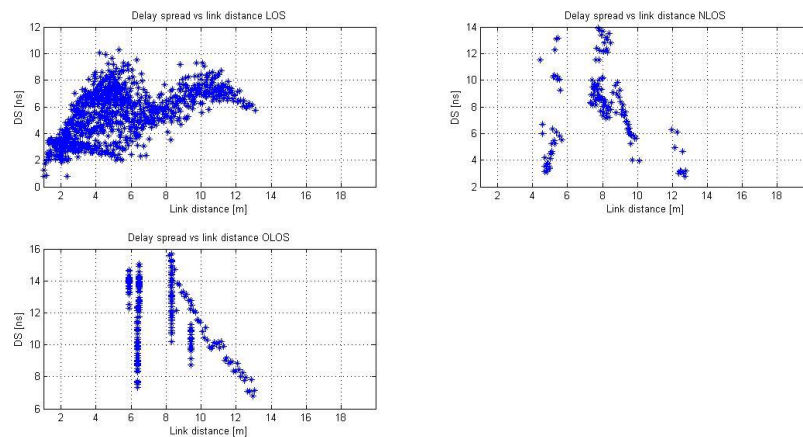
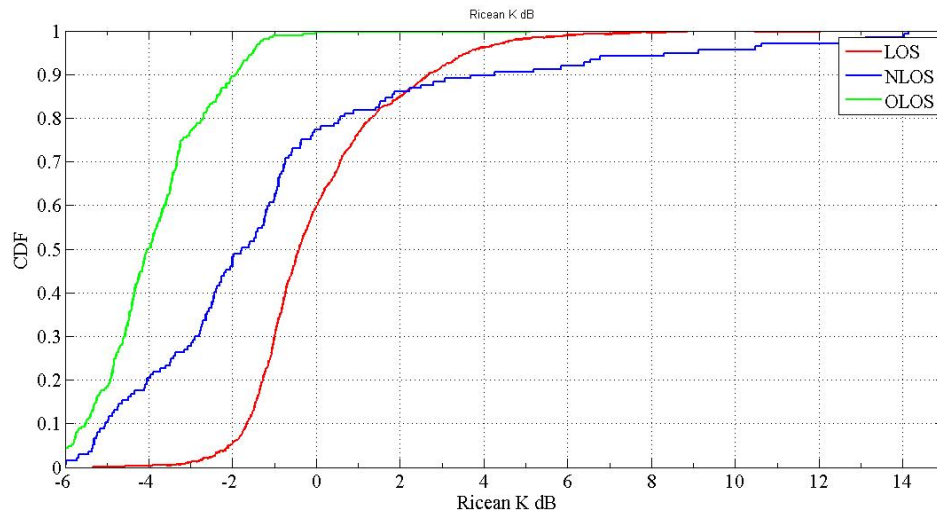


**Figure 6.2: RMS DS vs link distance.**

The observation of this work can be verified by the results reported in WINNER deliverable II. According to those results delay spread decreases for an increase in the frequency. The fact that reduction in the delay spread with an increase in frequency is valid in our case as well. It must be noted that in 60 GHz communication most of the communication is through LOS, which will lead to reduction in delay spread values in LOS case. Therefore, small delay spread values in LOS case is observed.

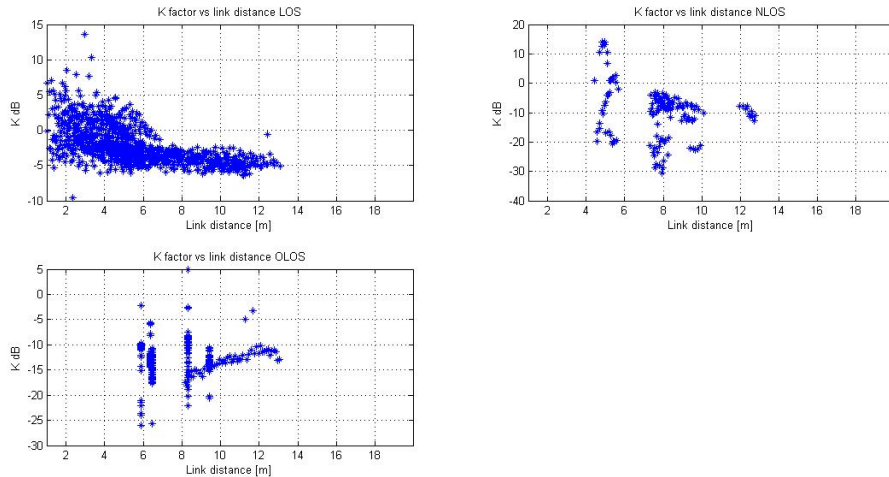
## 6.2. K-factor

The CDF plot of Rican K-factor for indoor cafeteria (LOS, NLOS and OLOS) is shown in Figure 6.3. We can observe that there is severe fading in all three cases as the values of  $K < 0$  and thus this indicates that there is severe fading at 60 GHz. The plot show that Rican K dB values for LOS case is higher as compared to OLOS and NLOS.



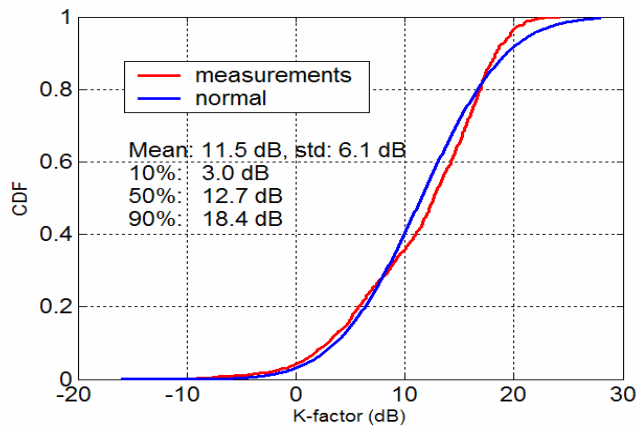
**Figure 6.3:** A CDF comparison in LOS, NLOS and OLOS cases of Indoor cafeteria.

Figure 6.4 shows the Rican K factor in dB as a function of link distance. In LOS the value of Rican K-factor is higher at small link distance and it decreases with increase in link distance. Almost same trend is also observed in NLOS and OLOS cases. We can make analysis that Rican K-factor increase in the case of LOS or in the absence of objects. Therefore, in LOS case high Rican K factor values are observed and smaller values are observed in OLOS and NLOS cases.



**Figure 6.4: Rician K dB vs. link distance.**

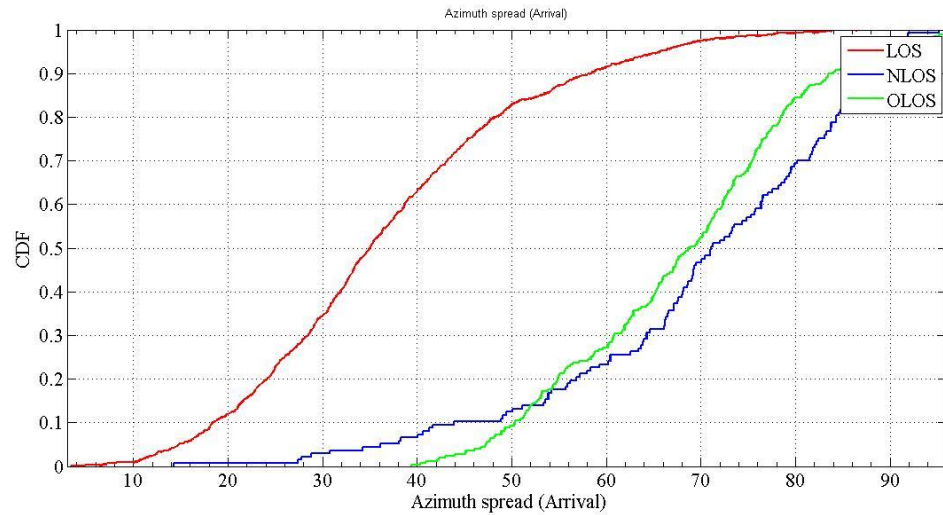
Figure 6.5 shows CDF plot of Rician K factor for *A1: Indoor* environment at 5.25 GHz center frequency for LOS case. Comparing the K factor values at 60 GHz with lower frequencies shows that K factor values at 60 GHz are smaller it is because when 60 GHz LOS path is blocked by some object then severe fading is observed as compare to lower frequencies.



**Figure 6.5: K-factor CDF plot of Indoor environment at 5 GHz [23].**

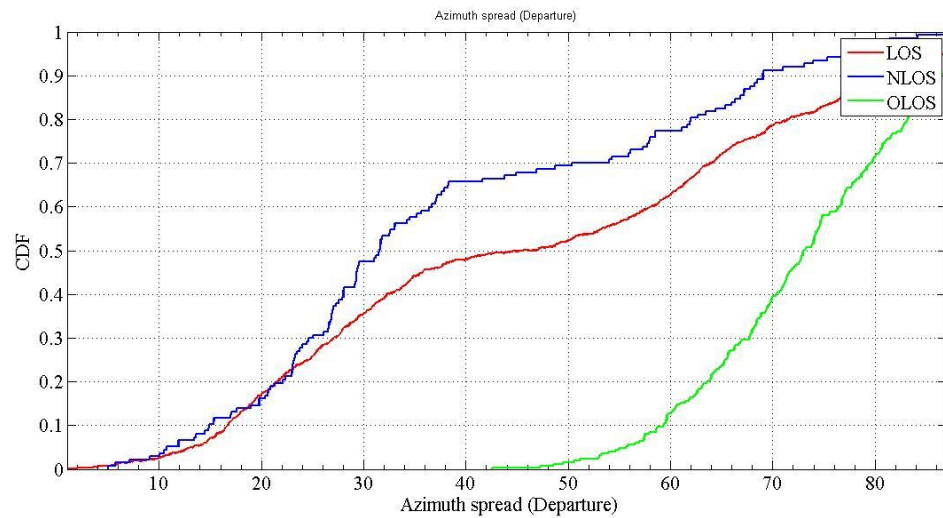
### 6.3. Azimuth angular spread (Arrival/Departure) Comparison

The azimuth angular spread is characterized both at TX and RX. Since at 60 GHz, most of the energy is carried through LOS signal path, therefore, we observed large value of azimuth spread in OLOS case. Larger value of angular spread indicates that more multi-path components are present in the environment. Hence, there are more multi-path components in OLOS case as compared to LOS and NLOS. Figure 6.6 shows CDF plots of angular spread (Arrival).



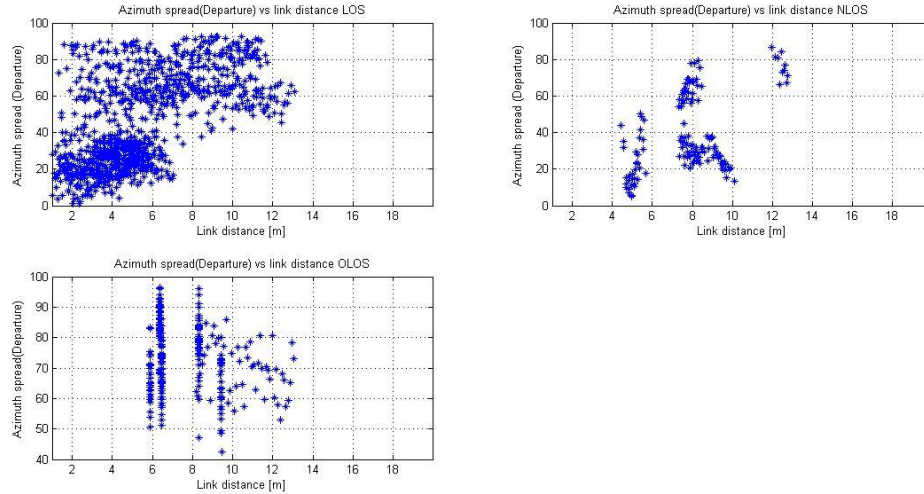
**Figure 6.6: Azimuth angular spread (Arrival).**

Figure 6.6 shows CDF plots of angular spread (Departure), it clearly shows that angular spread is higher in OLOS and NLOS cases.



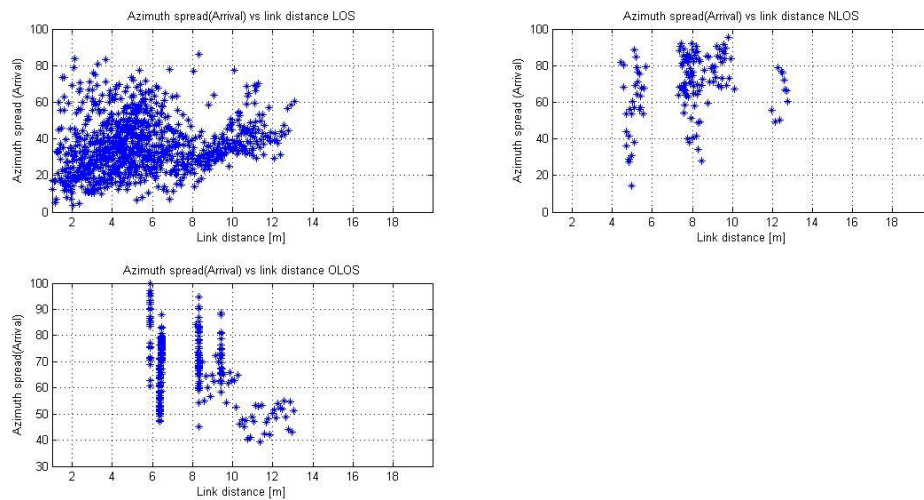
**Figure 6.7: Azimuth angular spread (Departure).**

Figure 6.8 shows azimuth spread (departure) as a function of link distance. The azimuth spread (departure) increases as the link distance increases which indicate that increasing link distance will add more multi-path component in the environment.



**Figure 6.8: AOD azimuth spread vs. link distance.**

Figure 6.9 shows azimuth spread (Arrival) as a function of link distance. The azimuth spread (arrival) also increases as the link distance is increased. Furthermore, larger value of angular spread indicates less correlation between the transmitter and receiver antennas.



**Figure 6.9: AOA azimuth spread vs. link distance.**

Furthermore, by comparing the values of azimuth spread at 60 GHz scenario with *AI: Indoor* scenario by analyzing table 6.1, we can make observation that azimuth spread is not large at 60 GHz compare to lower frequencies. It is because angular spread depends on the number of object in the environment, and the measurements at 60 GHz were performed in the absence of objects or humans, which leads to reduction in the angular spread. In addition, angular spread is small in LOS case as compare to OLOS and NLOS. We observed smallest azimuth spread value in LOS outdoor square and highest in OLOS and LOS cases of the indoor cafeteria.

#### 6.4. Elevation angular spread (Arrival/Departure) comparison

In order to give a full 3D channel model, the elevation parameters for WINNER channel model are derived. We can observe in Figure 6.10 and 6.11 that in NLOS and OLOS cases, there are more contributions of multi-path components, which lead to smaller elevation spread in LOS case and similar trend was observed in the azimuth parameters analysis.

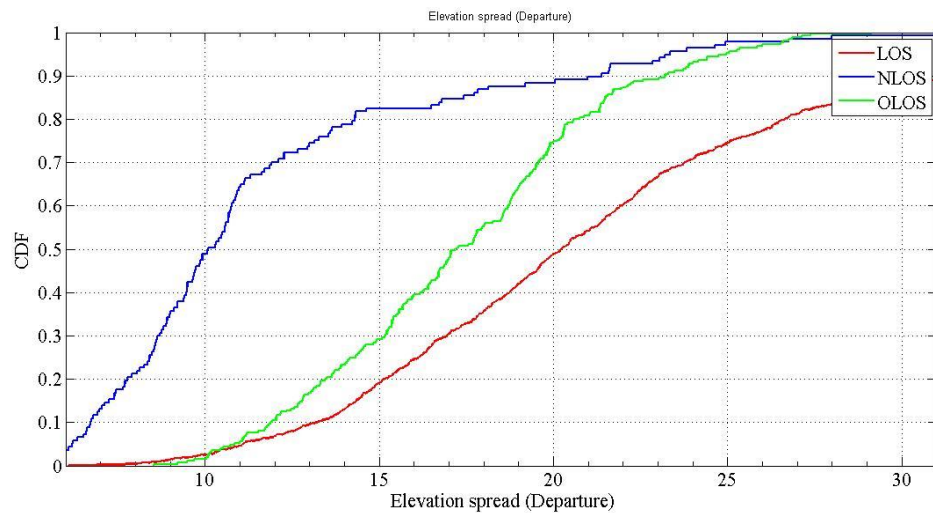


**Figure 6.10: Elevation spread (Departure).**

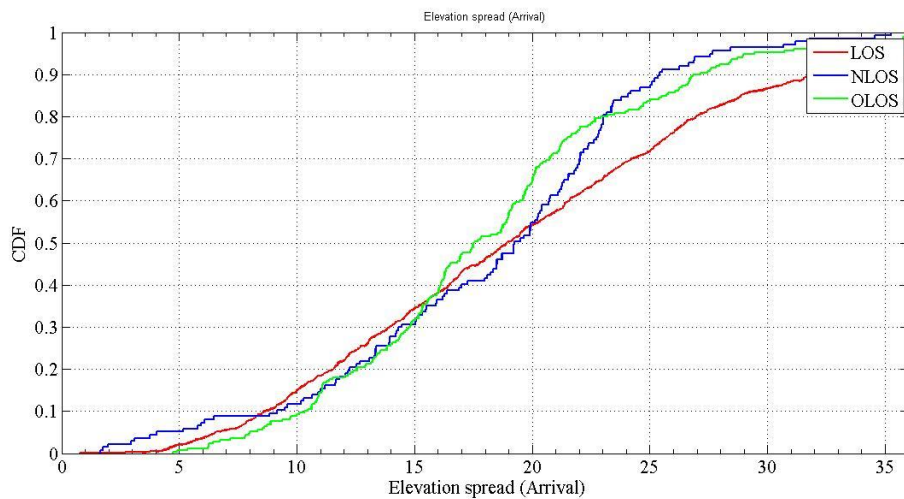


**Figure 6.11: Elevation spread (Arrival).**

Elevation spread as a function of link distance is plotted in Figure 6.12 and Figure 6.13. It can be observed that when the distance increases, the elevation spread (departure/arrival) decreases.

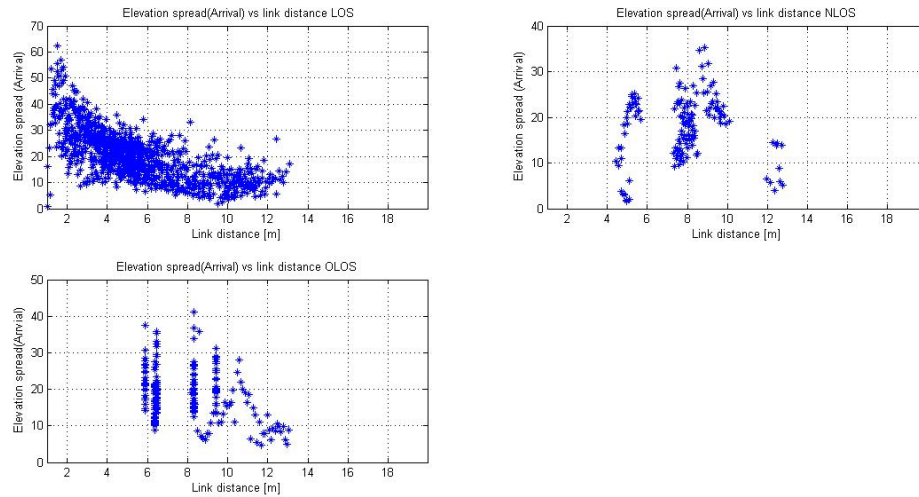


**Figure 6.10: Elevation spread (Arrival) versus link distance.**

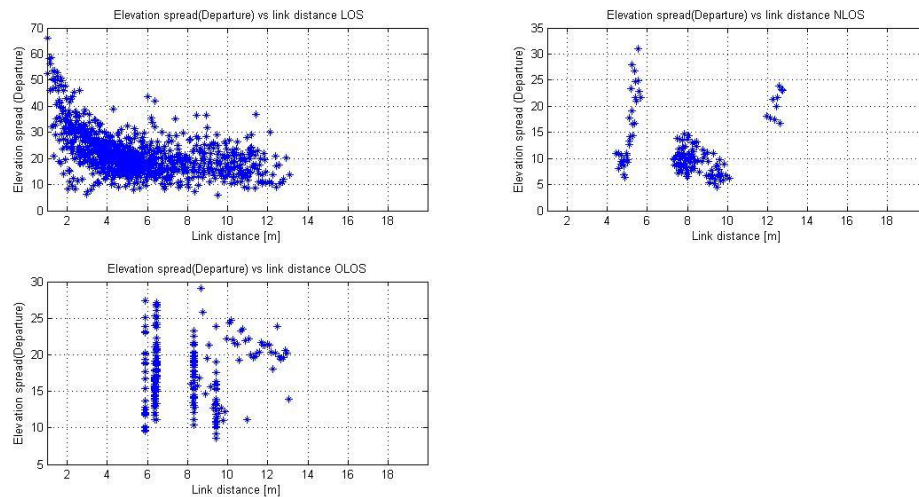


**Figure 6.11: Elevation spread (Departure) versus link distance**

Comparing the values of elevation spread at 60 GHz scenario with *A1: Indoor* scenario, we observed smallest elevation spread value in LOS outdoor square and highest in OLOS and LOS cases of the indoor cafeteria.

## 6.5. Number of clusters comparison

Many 60 GHz reports have different findings for the number of clusters. This difference in the finding is due to a number of factors such as measurement's bandwidth, number of objects in the environment. Higher bandwidth provides higher resolution that can resolve

more multi-path components, which can cluster more easily as they propagate in the channel.

It can be observe from the Figure 6.12 that the number of clusters is larger in OLOS case as compared to LOS and NLOS case. This is due to the reason that number of objects affects the number of clusters. The larger the number of objects within the environment, higher will be the number of clusters.

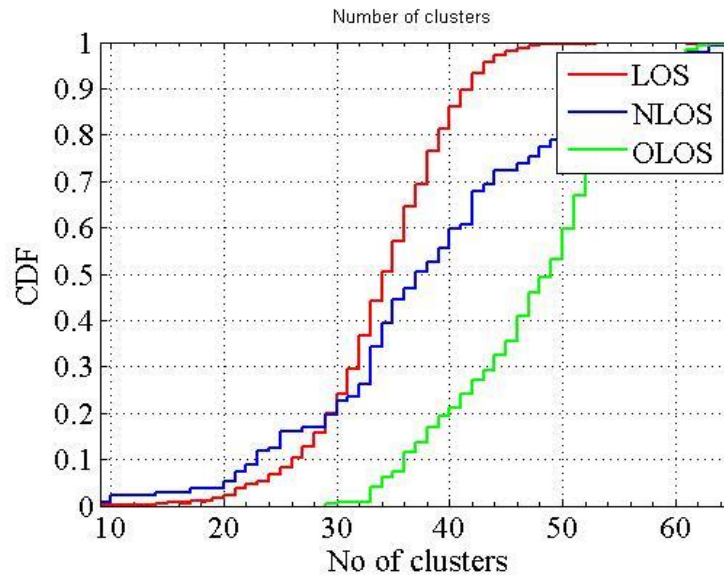


**Figure 6.12: Number of clusters.**

At 60 GHz, due to high bandwidth, there will be more number of clusters as compared to the number of clusters at lower frequencies. Which is true if we compare the number of cluster in *A1: indoor* environments with the environment at 60 GHz, we can observe that number of cluster are less at lower frequencies.

## 6.6. Path loss and shadow fading

The measured path loss and the path loss models for indoor cafeteria with LOS, NLOS and OLOS at 60 GHz are shown in Figure 6.13. The highest path loss can be seen in the NLOS case. Generally, path-loss at 60 GHz is high as compare to path-loss at lower frequencies. This is because path-loss at 60 GHz is subject to more losses due to absorption and rain attenuation. This makes real challenge in delivering a high data with reliable link margin. Therefore, the 60 GHz is a suitable candidate for indoor environment rather than outdoor.

Shadow fading component  $\sigma$  in Figure 6.13 indicates that the average power is larger or smaller than the local mean, respectively, and it is higher in OLOS case due to the fact that number of object increases the value of shadow fading.

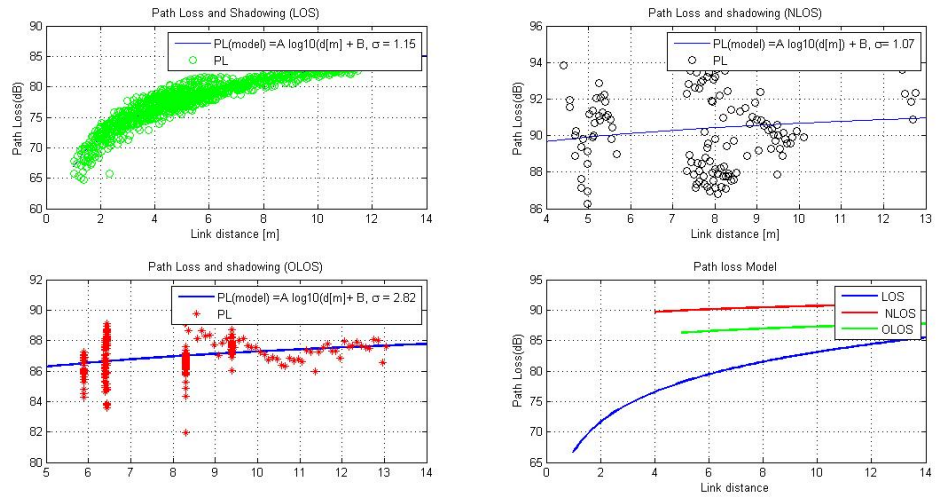


Figure 6.13: Path loss measurements and models for the indoor cafeteria scenario.

Figure 6.14 shows the path loss and path loss model for A1: Indoor environment, path-loss is smaller in LOS case as compare to NLOS case. In addition, path loss increases as the size of environment increases or when the distance between transmitter and receiver is large. Comparison of shadow fading values of the environment consider at 60 GHz and environment consider at lower frequencies, proves the fact that shadow fading depends on number of objects in the environment and directivity of antenna.

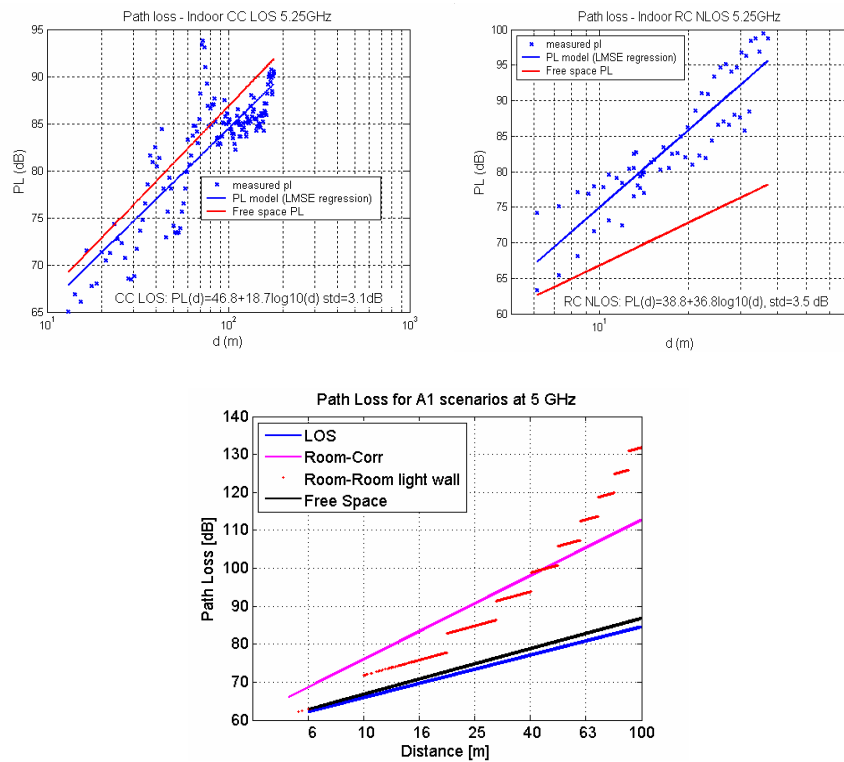


Figure 6.14: Path loss and path loss model for A1: indoor [23]

## 7. CONCLUSIONS

This thesis was started by introducing the basic concepts of radio propagation in order to develop the background knowledge about the radio propagation. After this, a literature review on channel modeling concept and radio propagation at 60 GHz was given. In this, review, deterministic model and stochastic models were briefly described together with some popular examples from these model types. Furthermore, needs of future channel models for mm-waves systems were identified. Especially what is missing in the current 60 GHz channel models?

The work continued by introducing the WINNER channel model and reviewing the work related to it. Further, the description about measurement equipment and sounder configuration was presented. In addition, the description about the environments considered in this work was presented. Before starting with the results and analysis, we introduced WINNER parameters in order to build knowledge about those parameters.

To conclude the work, a complete set of WINNER model parameters was presented for both indoor cafeteria and outdoor square scenarios. It was also considered especially interesting to investigate how the parameters are changed when the frequency is increased to 60 GHz. The result of this work are useful to produce the channel model at 60 GHz. This thesis contributes to an increased understanding of wireless propagation channel at 60 GHz, and the results of this thesis are useful in the design and development of future wireless systems in the mm-wave range.

For the future work, the channels can be reproduced from the WINNER II model using our derived parameters in order to show agreement with the channel generated from real time measurements in terms of parameters mentioned in this work. Apart from WINNER channel model, other channel models can be parameterize for the 60 GHz, and the output of those channel models can be compared with the WINNER model. This comparison will give clear idea that which channel model produces most reliable results and whether those results are enough to fulfill the requirements of prospective 5G networks. In addition, there is a need to perform channel measurements in complex and over-populated environments, e.g. football stadium, and develop channel models for those complex environments. Furthermore, there is also need for channel models for the hilly and mountainous areas.

## REFERENCES

- [1] S.K.Yong, P. Xia and A. Valdes-Garcia, Eds., *60 GHz technology for GBPS WLAN and WPAN from theory to practice*, Chichester, UK: Wiley, 2011.
- [2] A. Maltsev, R. Maslennikov, A. Sevastyanov, A. Lomayev, A. Khoryaev, "Statistical channel model for 60 GHz WLAN systems in conference room environment," in *2010 Proceedings of the Fourth European Conference on Antennas and Propagation (EuCAP)*, pp.1-5, 12-16 April 2010.
- [3] A. Deshmukh, S.K. Bodhe, "Characterization of radio propagation at 60 GHz channel," *First Asian Himalayas International Conference on Internet, 2009*. AH-ICI 2009, vol.1, no. 8, pp. 3-5, Nov. 2009.
- [4] C. Gustafson, "60 GHz wireless propagation channels: characterization, modeling and evaluation," Ph.D. dissertation, Dept. of Elect. and Information Technology., Lund Univ., Sweden, 2014.
- [5] T. Jämsä, P. Kyösti and K. Kusume, Eds., "Initial channel models based on measurements", *ICT-317669 METIS Deliverable D1.2*, Apr. 2014. [Online]. Available: <https://www.metis2020.com/documents/deliverables>
- [6] M. Döttling, Eds. *et al.*, *Radio technologies and concepts for IMT-advance*, Hoboken, USA: Wiley, 2009.
- [7] J. Järveläinen and K. Haneda, "Sixty gigahertz indoor radio wave propagation prediction method based on full scattering model", *Radio Sci.*, vol. 49, no. 4, pp. 293-305, 2014.
- [8] S.S. Hie, "Radio channel modeling for mobile ad hoc wireless networks," M.S. thesis, Naval postgraduate school, 2004.
- [9] M.L. Jakobsen, "Modeling and Analysis of Stochastic Radio Channels," Ph.D. dissertation, Dept. of Elect. Systems, Aalborg Univ., Denmark, 2013.
- [10] A. Arsal, "A study on wireless channel models: simulation of fading, shadowing and further applications," M.S. thesis, Dept. Elect. and elec.. Eng., Izmir Institute of Technology, Turkey, 2008.
- [11] S. R. Saunders and A. Aragón-Zavala, *Antennas and propagation for wireless Communication systems*, Chichester, UK: Wiley, 2007.
- [12] N. Blaunstein and C. Christodoulou, "Fundamentals of Radio Communications" in *Radio propagation and adaptive antennas for wireless communication links*, Hoboken, New Jersey:Wiley, 2007, pp.1-21.

- [13] GR. Lantero, "Statistical Channel Modeling Approach for Professional Wireless Microphone Systems" M.S. thesis, Institute of Radio frequency and Microwave Eng. Leibniz Univ., Hannover, Germany, 2010.
- [14] M. Zhu, "Geometry-based Radio Channel Characterization and Modeling: Parametrization, Implementation and Validation" Ph.D. dissertation Dept. of Elect. and Information Technology, Lund Univ., Sweden, 2014.
- [15] N. Jalden, "Analysis of Radio Channel Measurements Using Multiple Base Stations" Ph.D. dissertation, Dept. of Elect. Eng., KTH Univ., Stockholm, Sweden, 2007
- [16] P. Kyösti *et al.* (2007), *WINNER II Channel models, Part I Channel Models, Deliverable D1.1.2, V1.2* [Online].: <https://www.ist-winner.org/WINNER2-Deliverables/D1.1.2v1.1.pdf>
- [17] T. Brown, E. DeCarvalho and P. Kyritsi, *Practical guide to the MIMO radio channel with MATLAB examples*, Chichester, West Sussex, U.K: Wiley, 2012.
- [18] A. Molisch, *Wireless communications*, Chichester, UK: Wiley, 2005.
- [19] S. Salous, *Radio propagation measurement and channel modeling*, UK: Wiley, 2013.
- [20] M. Kyrö, "Radio wave propagation and antennas for millimeter-wave communications", Ph.D. dissertation, Dept. of Radio Science and Eng., Aalto University, 2012.
- [22] A. Karttunen, J. Jarvelainen, A. Khatun, K. Haneda, "Radio Propagation Measurements and WINNER II Parametrization for a Shopping Mall at 60 GHz," in *IEEE 81<sup>st</sup> Vehicular Technology Conference (VTC Spring)*, pp.1-5, 11-14 May 2015.
- [23] P. Kyösti *et al.* (2007), *WINNER II Channel models, Part II Channel Models, Deliverable D1.1.2, V1.0 Radio channel measurement and analysis results* [Online]. Available: <http://projects.celtic-initiative.org/winner+/deliverables.html>
- [24] K. Haneda, J. Järveläinen, A. Karttunen, M. Kyrö, J. Putkonen, "Indoor short-range radio propagation measurements at 60 and 70 GHz," in *8th European Conference on Antennas and Propagation (EuCAP)*, vol. 6, no. 11, pp.634-638, 6-11 April 2014
- [25] V. Degli-Esposti, F. Fuschini, E. M. Vitucci and G. Falciasecca, "Measurement and modeling of scattering from buildings", in *IEEE Transactions on Antennas and Propagation*, Vol 55 no 1, pp 143-153, 2007.
- [26] J. Järveläinen, M. Kurkela, A. Karttunen, K. Haneda and J. Putkonen, "70 GHz Radio Wave Propagation Prediction in a Large Office", in *Proc. 10th Loughborough Antenna & Propagation Conference (LAPC2014)*, Loughborough, UK, 2014.

- [27] M. Kyro, K. Haneda, J. Simola, K. Nakai, K. Takizawa, H. Hagiwara and P. Vainikainen, 'Measurement Based Path Loss and Delay Spread Modeling in Hospital Environments at 60 GHz', in *IEEE Transactions on Wireless Communications*, vol. 10, no. 8, pp. 2423-2427, 2011.
- [28] M. Ibnkahla, *Signal processing for mobile communications handbook*. Boca Raton: CRC Press, 2005.
- [29] S. Geng, J. Kivinen and P. Vainikainen, "'Propagation characterization of wideband indoor radio channels at 60 GHz', in *Microwave, Antenna, Propagation and EMC Technologies for Wireless Communications*, vol. 1, 2005.
- [30] L. Greenstein, D. Michelson and V. Erceg, 'Moment-method estimation of the Ricean K-factor', in *IEEE Communications Letters*, vol. 3, no. 6, pp. 175-176, 1999.
- [31] B. Clerckx and C. Oestges, *MIMO wireless networks channels, techniques and standards for multi antenna, multi users and multi cell systems*. 2<sup>nd</sup> edition, Academic press, 2013.
- [32] A. Goldsmith, *Wireless communications*, Cambridge Univ. press, UK, 2005.